Physicochemical Properties of the Alligator Lizard Tectorial Membrane

by

Henry E. Chung

Submitted to the Department of Electrical Engineering and Computer Science
in Partial Fulfillment of the Requirements for the Degrees of

Master of Engineering in Electrical Engineering and Computer Science
and
Bachelor of Science in Electrical Engineering

at the

MASSACHUSETTS INSTITUTE OF TECHNOLOGY

May 1994

Author.....
Department of Electrical Engineering and Computer Science
May 16,1994

Certified by.....
ennis M. Freeman
Research Scientist
Thesis Supervisor

Accepted by.....
c R. Morgenthaler
Professor of Electrical Engineering
Chairman, Departmental Committee on Graduate Students

Physicochemical Properties of the
Alligator Lizard Tectorial Membrane

by

Henry E. Chung

Submitted to the Department of Electrical Engineering and Computer Science

May 16, 1994

in Partial Fulfillment of the Requirements for the Degrees of
Bachelor of Science in Electrical Engineering and
Master of Engineering in Electrical Engineering and Computer Science

Abstract

This thesis project examines the osmotic properties of the unfixed alligator lizard tectorial membrane. The tectorial membrane is a microscopic and transparent inner ear structure that plays an important role in the transformation of sound into neural impulses.

Surgical procedures and experimental techniques were developed to isolate the tectorial membrane and to measure positions of microspheres affixed to the surface of the tectorial membrane using a Nomarski video microscopy system integrated with a perfusion system and an automated point-tracking program. This allowed us to examine changes in size, shape and structure of the tectorial membrane in response to isosmotic solutions of varying composition.

When the tectorial membrane was exposed to high-Na^+ solutions, swelling was observed. Comparable magnitude deswelling occurred on return to a high-K^+ solution. Minute reductions in Ca^{2+} concentration resulted in swelling responses even greater than those associated with predominant cation changes. The swelling responses were found to be reversible upon addition of Ca^{2+}. The swelling and shrinking behavior of the tectorial membrane was found to be isotropic and characteristic changes in the tectorial membrane microstructure were associated with changes in dimensions. These results, except for isotropism, are qualitatively consistent with those previously obtained from isolated avian and mammalian tectorial membranes.

The osmotic responses of the tectorial membrane to variations in K^+, Na^+ and Ca^{2+} concentration are of physiological interest because the concentrations of these ions are known to be regulated *in situ*. The results also have important implications for the micromechanics of the inner ear.

Thesis Supervisor: Dennis M. Freeman
Title: Research Scientist, Research Laboratory of Electronics

Acknowledgments

I would like to dedicate this thesis to my father and mother, Sang Jin and Sung Sook Chung, and to my sister Debbie. Without your love and support, I wouldn't even be close to where I am today.

I wish to thank my thesis advisor, Denny Freeman for taking on a undergraduate so many years ago, and seeing me through. I couldn't have asked for a better advisor and a friend. Thanks for everything, Denny!

I would also like to thank the other members of my research group, Professor Tom Weiss, "Dr." Quentin "Putah" Davis, Cam "Lowfat" Abnet, and Devang "Da Vangmeister MD" Shah for making Bldg. 36, 8th floor a great place to be.

A special thanks to Cam Searle for giving me the chance to participate in the Master of Engineering program and to Al Grodzinsky, who was my faculty advisor for all these years.

And last, but not certainly the least, I would also like to thank all of the friends that I have made at MIT. Thanks to all of you for making my time here fun, interesting, educational, and sometimes difficult, but never boring.

Contents

Chapter 1: Introduction

The tectorial membrane is a gelatinous structure that overlies the sensory receptor cells in the inner ear. Biochemical composition studies have shown that the tectorial membrane contains the important chemical constituents of a polyelectrolyte gel, similar to that found in connective tissues [7, 8, 17, 20, 24, 28, 29]. A polyelectrolyte gel consists of a network of macromolecules, ionizable fixed charges, mobile ions, and a high percentage of water [27]. The mobile ions can alter the state of the fixed charge groups in the network and thereby affect the osmotic pressure of the gel. This change in osmotic pressure results in the flow of water into or out of the gel, thereby altering its size, shape and mechanical properties. We call this the *osmotic response* even though it can occur in response to isosmotic changes in solution composition [4, 22]. To understand the tectorial membrane's properties and its auditory role, we need an understanding of its biochemical, mechanical, electrochemical, and osmotic properties [4, 6, 27].

The purpose of this study is to examine the osmotic responses of the isolated tectorial membrane. A variety of surgical procedures were developed to isolate the tectorial membrane of the alligator lizard. Changes in size and shape of the tectorial membrane were measured in response to various artificial lymphs.

1.1 Background

The tectorial membrane is an enigmatic structure found in the cochlear duct of most vertebrate animals. Its intrinsic properties make it difficult to study. The tectorial membrane is transparent, microscopic and easily disturbed or damaged. In the alligator lizard, the tectorial membrane is a two-part structure [15, 16]. The thick tectorial plate is located in close proximity to hair bundles of hair cells, and surrounds a number of them -- possibly contacting them. A much thinner veil-like structure extends away from the thick tectorial plate portion. The veil bridges the gap between the basilar papilla and the neural limbus, and drapes over the neural limbus. The position of the tectorial membrane demands that it plays a crucial role in delivering sound-induced mechanical stimuli to the hair bundles; however, relatively little is known about

the method by which it does this. To gain a better understanding of its role in hearing, we have chosen to examine the tectorial membrane's physicochemical properties.

1.2 Anatomy of the Alligator Lizard Cochlear Duct

The inner ear contains solutions with radically different compositions [19, 25]. The sensory receptor cells are part of an epithelium that separates two solutions, endolymph and perilymph. Endolymph is a solution that has a high concentration of K^+, a low concentration of Na^+, and trace Ca^{2+}. Perilymph is a solution that has a high concentration of Na^+, a low concentration of K^+ and a hundred times more Ca^{2+} than endolymph. The tectorial membrane is one of several inner structures that are bathed in endolymph. Other inner ear structures, such as the basilar membrane, are bathed in perilymph. Some portions of the cochlear duct such as the vestibular membrane are exposed to both types of lymph.

Among land-based vertebrate animals, the cochlear duct was first well-developed in reptiles. The species of southern alligator lizards, *Gerrhonotus multicarinatus*, has been the subject of numerous auditory studies in the last three decades and the micromechanics of its inner ear and neural organization of its inner ear is among the best understood. Also, the structure of the basilar papilla and the overlying tectorial membrane possess relatively simple geometry in comparison the functional counterparts in mammals.

Structurally, the basilar papilla in the alligator lizard is attached to the basilar membrane and is roughly cylindrical in shape. This can be seen in Figure 1.1. It is approximately 400 μm in length, 30 μm high, and up to 40 μm wide [15]. The basilar papilla is divided into two morphologically distinct regions: the tectorial region and the free-standing region.

The tectorial region is approximately 150 μm in length and is primarily characterized by the presence of the tectorial membrane overlying and surrounding a number of short (< 10 μm) stereociliary bundles [3, 9, 15].

Adjacent to the tectorial region on the basilar papilla is the free-standing region that is approximately 250 μm in length. Stereociliary bundles in this region are free-standing and range in height from 30 μm at the tectorial-free-standing boundary, to 12 μm at its end. The free-standing region is widest at its midpoint and tapers to a narrow tip.

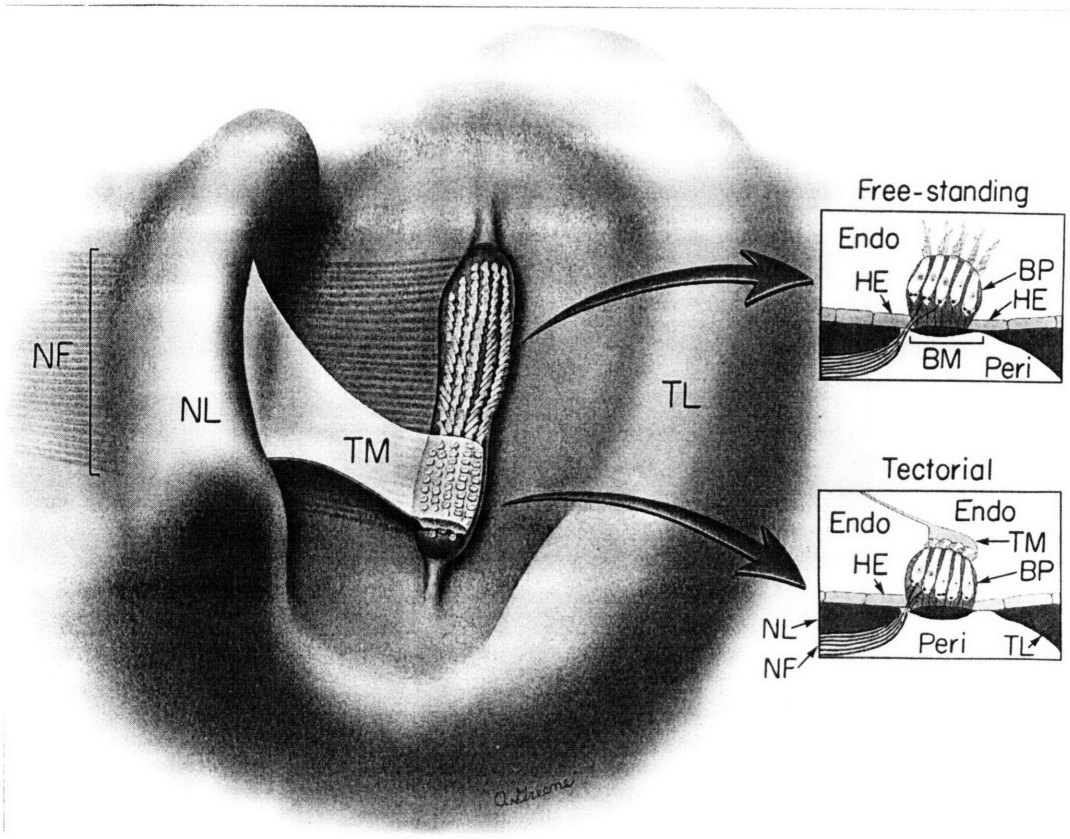

Figure 1.1: The endolymphatic surface of the alligator lizard cochlear duct.
This illustration (by Anne Greene) depicts the surface of the cochlear duct that is bathed in endolymph. Structures of interest are identified with abbreviations. Nerve fibers (NF), neural limbus (NL), tectorial membrane (TM), triangular limbus (TL), basilar papilla (BP), basilar membrane (BM), hyaline epithelial cells (HE), endolymphatic fluid space (Endo), perilymphatic fluid space (Peri).

The basilar papilla contains approximately 160 hair cell receptors, of which approximately 35 are found in the tectorial region, and 125 in the free-standing region. The hair cells form staggered rows in a lateral orientation. These rows contain 3 to 4 hair cells in the tectorial region, and between 3 and 6 hair cells in the free-standing region. In both cases, the number of hair cells in a row depends upon the width of the basilar papilla. The morphological polarization of the stereociliary bundles, which determines the directional sensitivity of mechanical transduction, also varies depending upon the region in which they are found [6, 11, 16, 30]. In the tectorial region, stereociliary bundles are oriented so that motions toward the triangular limbus are excitatory. In the

free-standing region, stereociliary bundles are oriented so that motions toward the midline of the basilar papilla excitatory [6, 11, 16, 30].

1.3 Organization of the Thesis

A description of the macrosurgery, microsurgery, solutions, and the experimental setup is given in Chapter 2, Methods. Results are given in Chapter 3, with discussion and implications of these results found in Chapter 4.

Chapter 2: Methods

The methods utilized in this study follow those used in a similar study of the unfixed chick tectorial membrane [4]. However, some modifications and improvements have been made to accommodate differences between the chick and the alligator lizard.

The tectorial membrane of the alligator lizard was surgically isolated and adhered to Cell-Tak, a cellular adhesive, to the bottom surface of an experimental chamber. Carboxylated microspheres (beads) were then affixed to the top surface of the tectorial membrane. These beads provided fixed points of reference and could be easily tracked as the tectorial membrane changed in size and shape. In addition, images providing insight into the structure of the tectorial membrane were also recorded at regular intervals.

2.1 Solutions

The compositions of artificial endolymph, perilymph and derivatives specified in Tables 2.1 and 2.2 are identical to those used in the previous chick study, except for the presence of 2 mM of potassium in the artificial perilymph and perilymph derivative solutions, as opposed to 3 mM [4]. This allowed for symmetry in comparing solutions with different predominant cation [22]. The codes used in identifying our solutions, such as artificial endolymph (K20) and artificial perilymph (Na2000) are composed of the chemical abbreviation of the predominant cation, followed by the micromolar (μM) concentration of calcium.

	K0	**K2000**	**KEGTA**
NaCl	2	2	2
KCl	174	171	173
$CaCl_2$	0	2	0
Dextrose	3	3	3
HEPES	5	5	5
EGTA	0	0	1
KOH	~2	~2	~4

All values are in mM (mmol/L)
All solutions @ pH = 7.30±0.005

Table 2.1: Composition of artificial endolymph and derivative solutions.
All solutions have K^+ as the predominant cation. High-K^+ solutions include K0 (low Ca^{2+}), K20 (AE, made by diluting K2000 with K0), K2000 (high Ca^{2+}) and KEGTA (with Ca^{2+} chelator). Solutions also include small amounts of KOH and HCl to adjust pH to 7.30±0.005

	Na0	**Na2000**	**NaEGTA**
NaCl	174	171	173
KCl	2	2	2
$CaCl_2$	0	2	0
Dextrose	3	3	3
HEPES	5	5	5
EGTA	0	0	1
NaOH	~2	~2	~4

All values are in mM (mmol/L)
All solutions @ pH = 7.30±0.005

Table 2.2: Composition of artificial perilymph and derivative solutions.
All solutions have Na^+ as the predominant cation. High-Na^+ solutions include Na0 (low Ca^{2+}), Na20 (made by diluting Na2000 with Na0), Na2000 (AP) and NaEGTA (with Ca^{2+} chelator). Solutions also include small amounts of NaOH and HCl to adjust pH to 7.30±0.005

Solutions containing added concentrations of calcium other than 0 or 2000 μM were produced by diluting stock solutions of K2000 and Na2000 with K0 and Na0 respectively.

The pH of all stock solutions was measured using an Orion triode pH electrode, model 91757 BN. For artificial endolymph solutions, 1M KOH and 1M HCl were used to adjust the pH to 7.30. For artificial perilymph solutions, 1M NaOH and 1M HCl were used to adjust the pH to 7.30.

No calcium was intentionally added to solutions of K0 or Na0. However, use of a calcium ion selective electrode (Orion model 9320) in a calcium ion titration suggests that a very low level of calcium is present in solution, less than 7 μM. After testing of the water, chemicals used, and instrumentation, the source of this low level calcium contamination has been determined to be the salts used in preparing the solutions. The KCl and NaCl salts were tested by the supplier (Sigma) to contain no more than 0.0015% Ca, which places a limit of no

more than 15 μM Ca^{2+} for our artificial lymph solutions. This is consistent with the Ca^{2+} ion-selective electrode results [4].

2.2 The Experimental Chamber

The experimental chambers used in this study were fabricated from standard glass microscope slides and rubber O-rings with 1 cm inside diameter. The O-rings and glass slides were rinsed in ethanol and the O-rings were mounted with 5 minute epoxy to produce a watertight seal. This produced a chamber with a 0.3 mL fluid capacity.

For each experiment, the chamber floor was swabbed and rinsed with detergent, acetic acid and water. One microliter of Cell-Tak was applied in the middle of the chamber by a micropipetor and spread out in a circular manner. The acetic acid in the Cell-Tak was then allowed to evaporate, leaving behind a thin layer of tissue adhesive ready to adhere to the cochlear duct and tectorial membrane.

2.3 Surgery

The surgical procedures involved in isolating a tectorial membrane can be divided into two distinct phases. The macrosurgery phase begins with the sacrifice of the alligator lizard and concludes with isolation of the cochlear duct. The microsurgery phase takes the isolated cochlear duct and concludes with the isolation of the tectorial membrane.

2.3.1 Macrosurgery

Adult alligator lizards vary in length from 15 to 30 cm, with variation depending primarily upon tail length. Similarly, typical weights range between 15-35 grams. However, the size of the cochlear duct and other inner ear structures vary little with the body size and weight of the adult alligator lizard.

Adult alligator lizards were anesthetized by refrigeration for 60-90 minutes then sacrificed by decapitation and immediately pithed. The skin and muscle dorsal and medial to the outer ear and posterior to the skull casing were removed using a scalpel, scissors, and forceps. The thin layer of bone above the sacculus was removed by short lateral motions of scalpel blade held flat. The

resulting hole was then enlarged, using a curette to expose the saccular otoconia. The saccular otoconia were flushed out by jets of artificial endolymph (K20) delivered by a syringe and needle. With the saccular otoconia removed, the cochlear duct and some of its structures were visible in a dissecting microscope. The eighth nerve was also visible at this point and was cut with a razor blade sliver where it exited the bony capsule surrounding the cochlear duct. The cochlear duct was then removed by picking up the cut end of the eighth nerve using fine forceps. The isolated cochlear duct was then transferred into a previously prepared experimental chamber, containing a layer of the cellular adhesive Cell-Tak (Collaborative Research Inc.) on the chamber floor and filled with filtered (Supor-450, Gelman Sciences) artificial endolymph (K20).

2.3.2 Microsurgery

An eyelash affixed to a glass capillary was used to press the cochlear duct down to the Cell-Tak coated floor. With the Cell-Tak adhering to the cochlear duct, a pair of fine forceps was used to grab the vestibular membrane in the tiny hole where the reunient duct connects the cochlear duct to the saccule. A quick peeling back along and above the triangular limbus would generally open the duct and provide clear access to the tectorial region of the basilar papilla.

With the vestibular membrane removed from above the tectorial membrane, a tungsten probe could be used to remove the tectorial membrane by its veil. This probe was fabricated by repeated flaming of a fine tungsten wire until its end diameter was reduced to 15 μm. The probe was manually placed in the space between the neural limbus and the basilar papilla and slid beneath the veil portion of the tectorial membrane. The probe was then carefully lifted up along the neural limbus, detaching the veil from its neural limbus connection and affixing itself to the probe. The tectorial membrane could then be carefully lifted off the basilar papilla by its veil and placed upon the Cell-Tak. All other components of the cochlear duct and debris were then removed.

Carboxylated latex microspheres, referred to henceforth as "beads", with diameters of 2.01 μm were diluted 1:10 with filtered K20. This solution of beads was sonicated and passed through 6 layers of filter paper (Whatman Qualitative #1) to separate bead clusters and 10 μL was delivered manually to the tectorial membrane by a 100 μL glass syringe. If 10-15 beads were not visibly settled on the tectorial membrane or 5-10 beads were not visible on the Cell-Tak coated

chamber floor in the microscope field of view, another 10 μL of the bead solution was delivered. This process was repeated until the target number of beads was reached as seen in Figure 2.1, at which point the chamber was placed on the stage of the Zeiss Standard WL compound microscope.

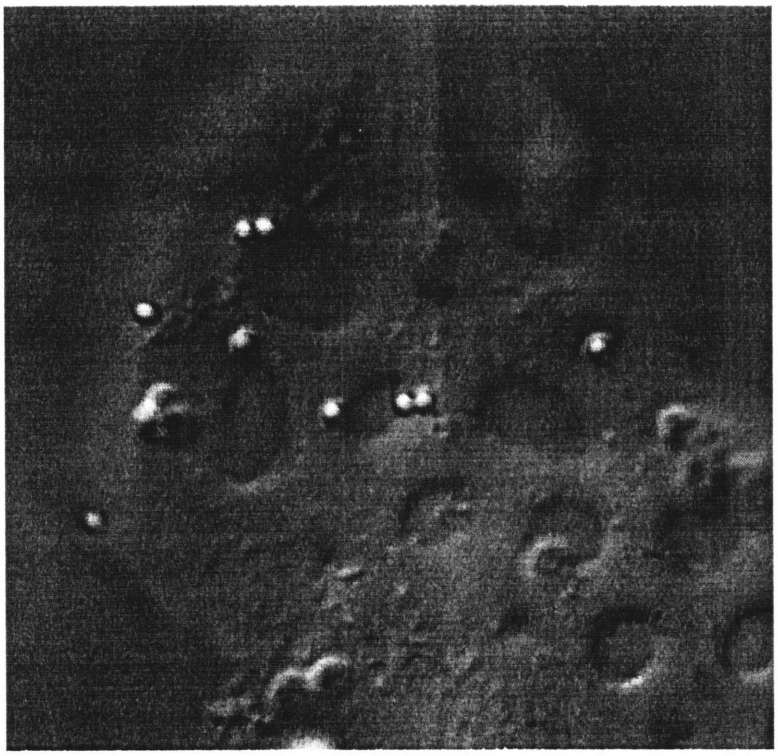

Figure 2.1: Tectorial membrane with carboxylated microspheres affixed.
This image illustrates a section of an isolated tectorial membrane with beads stuck to its surface. Under Nomarski microscopy, beads appeared as bright spheres and functioned as excellent positional landmarks.

2.4 The Experimental Setup

There were two primary subsystems to the experimental setup (Figure 2.2), the video microscopy subsystem, which recorded positional data and images, and the perfusion subsystem, which delivered the different perfusates into the experimental chamber in a stable manner.

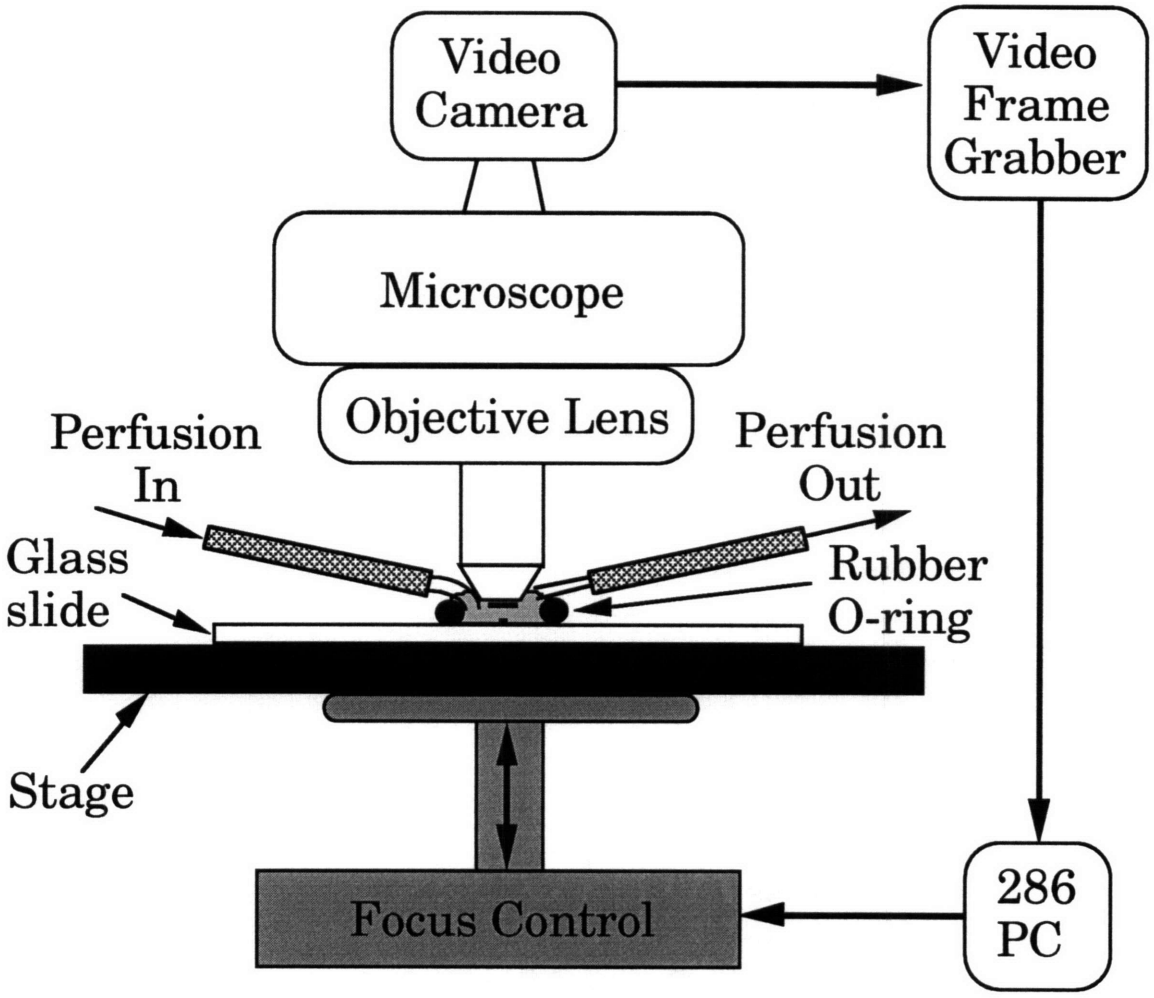

Figure 2.2: Schematic diagram of the experimental setup.
This diagram illustrates the key aspects of the experimental setup such as the video microscopy subsystem, the perfusion subsystem and the experimental chamber (defined by the rubber O-ring and the glass slide). The video microscopy subsystem includes the video camera, the video frame grabber, the 286 PC computer and the stepper-motor driven fine focus control, which raises and lowers the stage. A perfusion subsystem delivered fluid into and out of the experimental chamber. The experimental chamber was where the tectorial membrane was isolated and bathed in different ionic solutions.

2.4.1 The Video Microscopy Subsystem

The video microscopy system consisted of a Zeiss Standard WL compound microscope with its fine focus outfitted for automated, stepper-motor control. The optics of the microscope were set up for differential interference contrast (Nomarski) microscopy using a 40X water-immersion lens, and an optivar providing 2X magnification. The resultant images were captured by a Hamamatsu C2400 video camera, then digitized by a Data Translation DT2862

frame-grabber in a 286-based PC compatible outfitted for bead-tracking and data storage. The images captured had a final magnification of 0.229 μm/pixel. The video camera output was also made visible on a video monitor and recorded on video cassette for later review.

2.4.2 The Perfusion Subsystem

The perfusion system consisted of two Razel A99 syringe pumps, one Rainin Rabbit-Plus peristaltic pump and Teflon tubing. The two syringe pumps were dedicated for test solution influx into the chamber and the peristaltic pump was dedicated for efflux of test solution out of the chamber. The pumps provided constant perfusion, and the ability to exchange test solutions non-disruptively. A 4-way valve in the influx pump system allows for pump priming, which reduced switching transients to less than 1 minute. Pumping rates were controlled so that the perfusion rate was maintained at 10 mL/hour.

Disposable, sterile 60 mL syringes were used in the syringe pumps. The syringes were filled with artificial lymphs and allowed to equilibrate to room temperature to prevent air bubbles from entering the perfusion system.

Perfusion intervals generally lasted between 30-60 minutes with the initial perfusion solution always being the same solution used during surgery, K20.

2.4.3 Perfusion into the Chamber

A supplemental stage was fabricated out of thin (2 mm) anodized steel, which renders it rustproof and ferromagnetic. The syringe pumps delivered test solutions through a 2 meter length of 1 mm inside diameter Teflon tubing. The tubing terminated into a blunt stainless steel needle. A small, high-strength rare earth magnet was epoxied to the needle to allow the needle unit to be magnetically anchored to the stage. Attached to the needle was a 2 cm length of 1 mm inside diameter silicone tubing terminated with a 1 cm length of glass capillary tubing that was bent for influx and straight for efflux. The effect of the silicone tubing-glass tubing attachment was to provide a more mechanically stable source of perfusion. The bend in the influx glass tubing ensured good mixing of the test solutions in the chamber, whereas the straight tubing provides

for a constant level of fluid in the chamber despite surface tension effects. This is illustrated in Figure 2.2.

2.5 Measurement Methods

Beads were used as 3-dimensional markers on the tectorial membrane and the experimental chamber floor. The video microscopy subsystem was limited to the tracking of 10 beads every minute. Therefore, two or three beads were located on the chamber floor for reference, and the rest were located on the tectorial membrane. All beads were automatically tracked by the PC-based programs BEADS and AUTOS. For each bead, 30x30x30 pixel cubes of frame-grabbed video were taken around the bead's last recorded position and analyzed to determine a new bead position.

The x and y coordinates for each bead were taken as pixel locations and later calibrated against a stage micrometer. The z coordinates, along the optical axis, were determined from optical encoder outputs capable of determining the extent the fine-focus control had been adjusted in order to focus upon each individual bead. The software autofocus routine was designed to search for the largest points of contrast in the 30 pixel vicinity of the previously determined location of the bead. The 30x30x30 pixel cubes and the estimated positions were stored every minute, and every 5 minutes full images in the plane of each bead were stored. At the termination of a typical 12 hour experiment, a total of a gigabyte of data had been collected.

The precision and accuracy of the entire measurement system were characterized by tracking 3 stationary beads affixed to Cell-Tak for several hundred minutes through a number of perfusion solution changes. These measurements test the stability and repeatability of automated bead position tracking. Figure 2.3 shows histograms of measurement noise in each of the three coordinate directions.

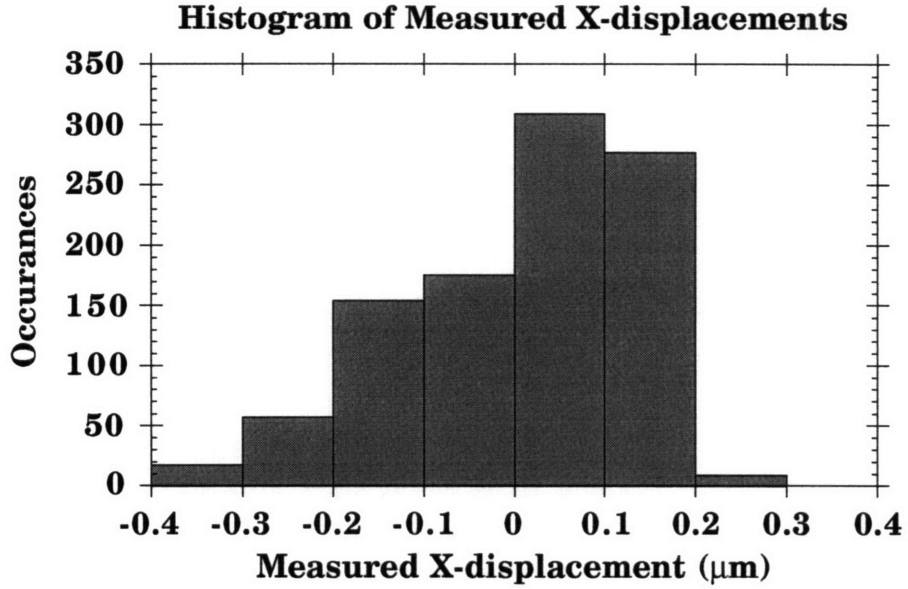
Histogram of Measured X-displacements
Occurances
350
300
250
200
150
100
50
0
-0.4
-0.3
-0.2
-0.1
0
0.1
0.2
0.3
0.4
Measured X-displacement (μm)

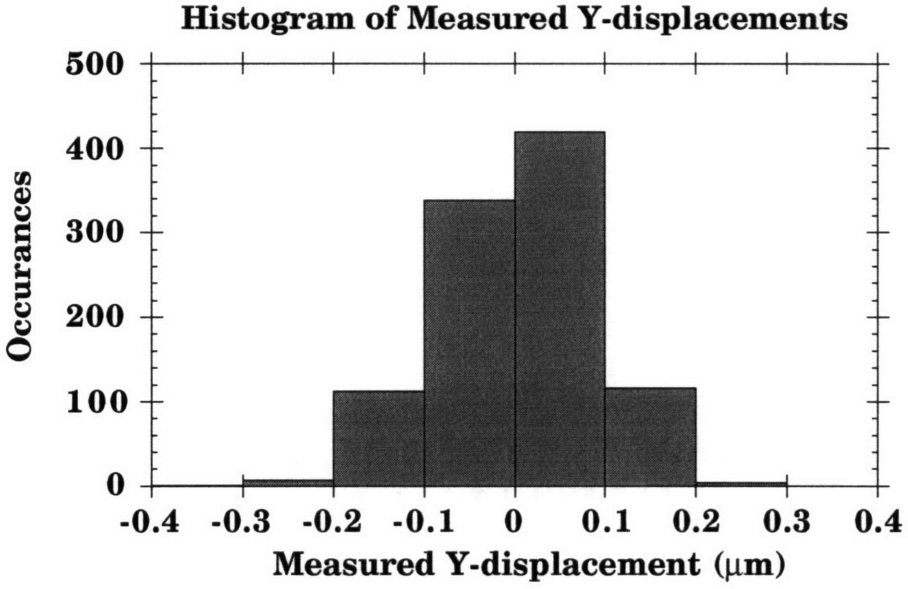
Histogram of Measured Y-displacements
Occurances
500
400
300
200
100
0
-0.4
-0.3
-0.2
-0.1
0
0.1
0.2
0.3
0.4
Measured Y-displacement (μm)

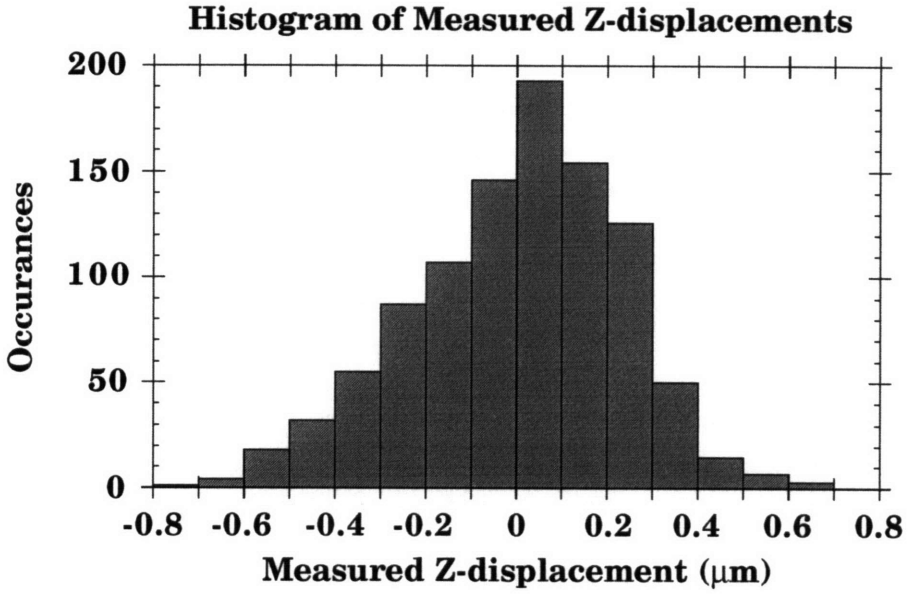

Figure 2.3: Static system verification for bead-tracking.
The histograms show 1000 independent measurements taken at one minute intervals of 3 beads affixed to the surface of a test chamber. The measurement noise along the three coordinate axes is reflected by the spread in the measured displacements. The standard deviation for measurement noise was 0.12 μm along the x-axis, 0.083 μm along the y-axis and 0.23 μm along the z-axis.

2.6 Animal Care

The care and use of alligator lizards in this study (supported with funds from NIH Grant #R01 DC00238) were approved by the Massachusetts Institute of Technology Committee on Animal Care.

Chapter 3: Results

Altering the ionic composition of the bath induced changes in the size and shape of the tectorial membrane. These changes are referred to as osmotic responses because we assume they must result from the transport of water into and out of the tectorial membrane [4, 22]. Since only isosmotic solutions were used in this study, any observed osmotic response is purely a result of changes in bath ionic composition.

We first examined artificial lymph changes between endolymph and perilymph. These solutions have radically different compositions and are found in close proximity *in situ*. To better understand the physicochemical basis of the osmotic responses to perilymph, we decomposed endolymph-perilymph exchanges into two separate changes: altering the predominant cation (K^+ and Na^+), and altering the Ca^{2+} concentration (20 μM or 2000 μM). This allowed us to ascribe certain effects to distinct ions and their concentrations.

The results described are obtained from 7 isolated tectorial membranes perfused with various artificial lymphs over a 48 hour period following surgical removal.

All summary plots in this section include all relevant data from each of the 7 preparations with the following exceptions.

Occasional problems with the perfusion system resulted in air bubbles or overflowing of the chamber and thereby led to intervals where the data were corrupted. There were several instances when beads were tracked inaccurately by the AUTOS program -- generally when other high contrast structures were within one diameter (2 μm) of the target bead. Lastly, there was one case where a bead was affixed to an unsecured underside part of a tectorial membrane, resulting in uninterpretable data.

Figure 3.1 illustrates results from a typical experiment with a number of intervals exchanging sodium and potassium at low and high calcium concentrations.

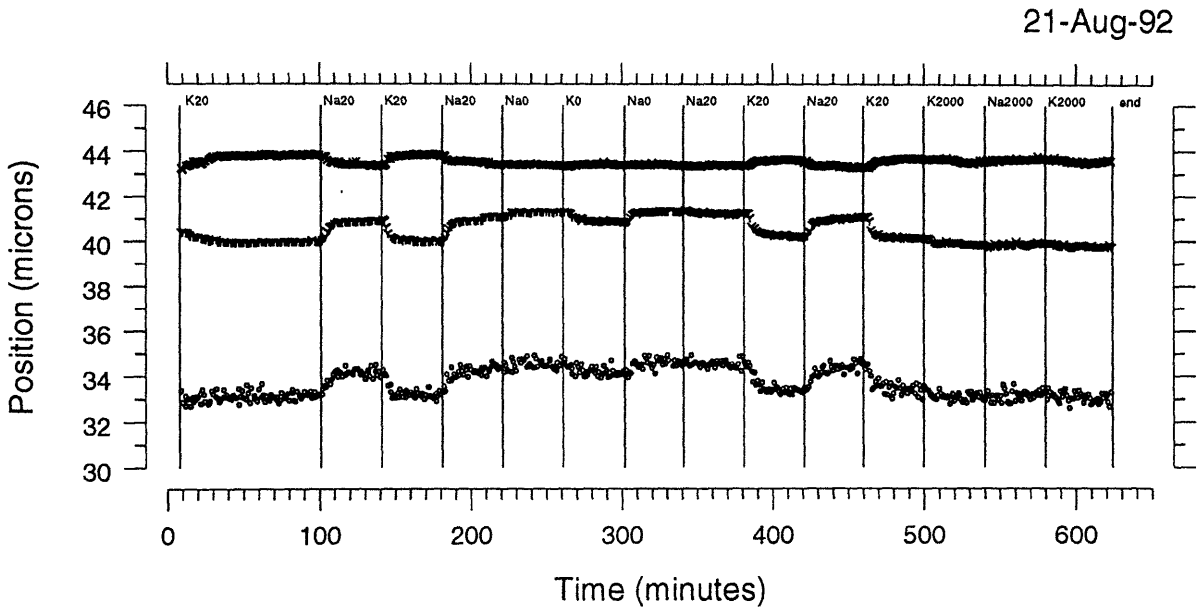

Figure 3.1: Bead tracking results from a typical experiment.
This plot shows bead position data recorded from a single bead over time during an experiment on the second day of a preparation. The symbols (X,Y,O) represent the position (X,Y,Z) of one bead taken every minute as a sequence of solutions were perfused. The vertical lines denote the times when the perfusates (enumerated by their codes along the top of the plot) were changed. The X and Y axes have been displaced so that the X and Y positions can be plotted on the same scale as z (thickness of the tectorial membrane).

Figure 3.1 clearly illustrates changes in the three-dimensional geometry of the tectorial membrane during a typical experiment. The time axis generally referred to elapsed time from the start of an experiment. The start of an experiment was either time of sacrifice of the lizard, or on the second day of an experiment, the time at which the bead-tracking program was restarted. A swelling response, seen in the z-axis (circles) at 100 minutes, is associated with a solution transition between K20 and Na20. We can also see that the response is composed of a transient followed by a stable plateau. The changes that occur in all three dimensions appear to follow an exponential curve. Hence, the positional data for each bead was fit with an exponential time function in order to extract magnitude and, in some cases, time constants. This is seen in Figure 3.2.

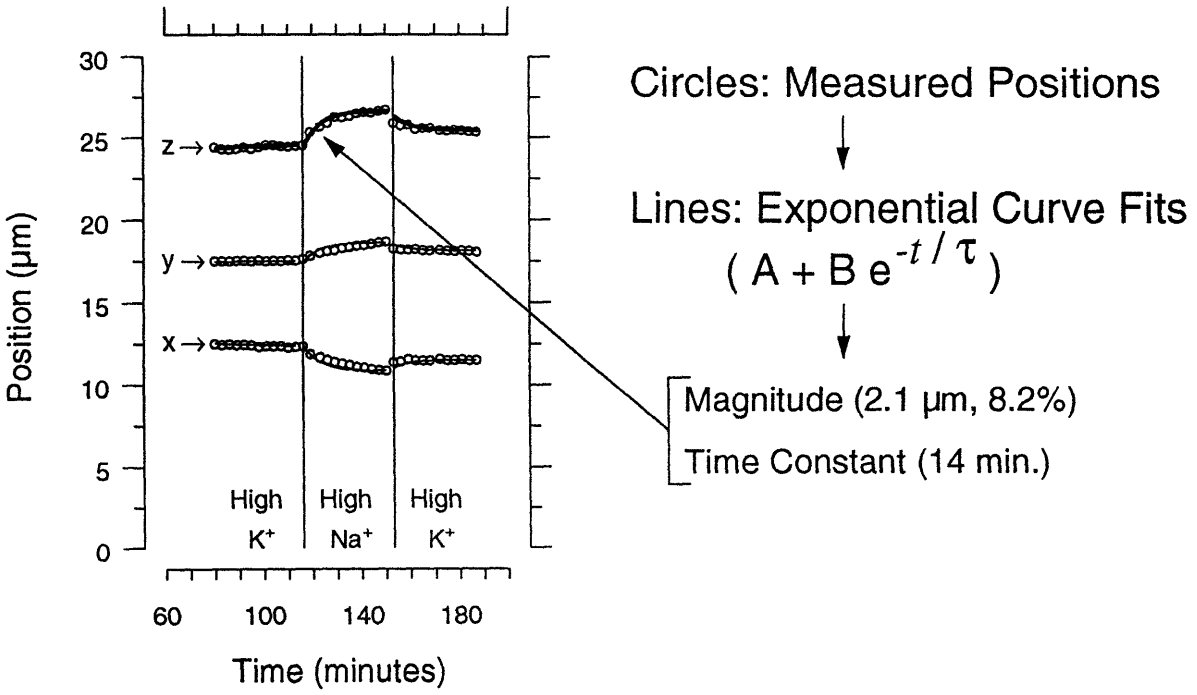

Figure 3.2: Exponential curve fit to bead position measurements.
This plot illustrates bead position measurements that were fitted with first-order exponential time functions in order to extract magnitude and time constant information.

Excursions along the z-axis directly represent swelling and deswelling of the tectorial membrane and are easily interpreted; however, changes in the x and y-axes are more difficult to interpret.

Analysis of images suggests that the tectorial membrane swells and shrinks along the outward normal of its surface. Figure 3.3 illustrates that beads on or near the edge of the tectorial membrane have the greatest absolute displacements in the x and y directions, whereas beads near the center of the tectorial membrane experience little or no absolute displacement in the x and y directions.

Because of the difficulty of interpreting bead excursions in the x and y directions, excursions along z-axis (swelling and shrinking) were examined initially.

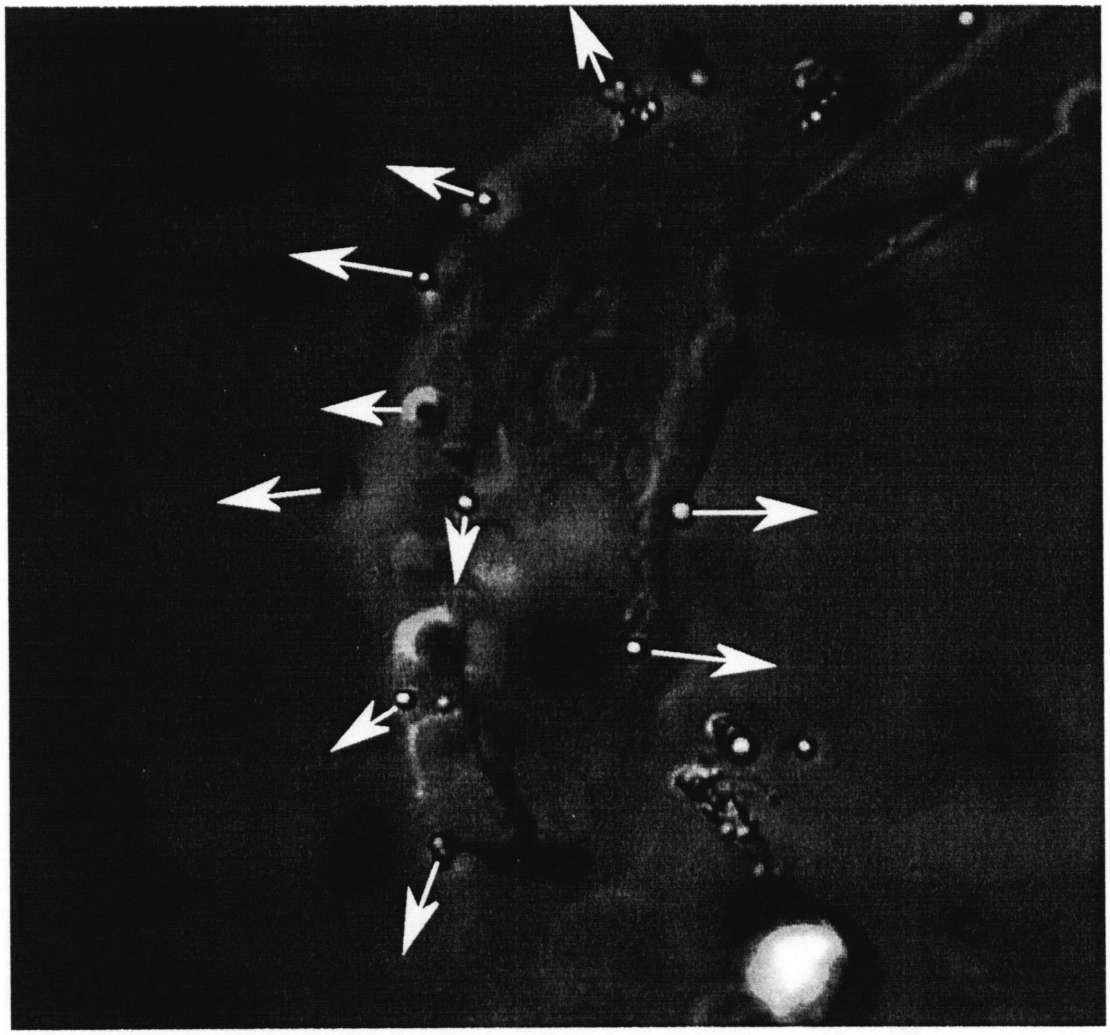

Figure 3.3: Tectorial membrane with beads affixed and resultant swelling pattern.
This image illustrates the outward normal expansion as the tectorial membrane swells. It shows the difficulty of interpreting X and Y axis bead position measurements, since absolute magnitude displacements depend on bead location on the tectorial membrane.

3.1 Effects of exchanging artificial endolymph and artificial perilymph

The inner ear contains two solutions with radically different compositions: endolymph and perilymph [26]. *In situ*, the tectorial membrane is bath predominantly with endolymph. To determine the effect of bathing the tectorial membrane in perilymph, we did experiments in which the solution bathing an

isolated tectorial membrane was alternated between artificial endolymph (K20) and artificial perilymph (Na2000).

Figure 3.4 and Table 3.1 summarize the excursions along the z-axis for transitions between artificial endolymph (K20) and artificial perilymph (Na2000).

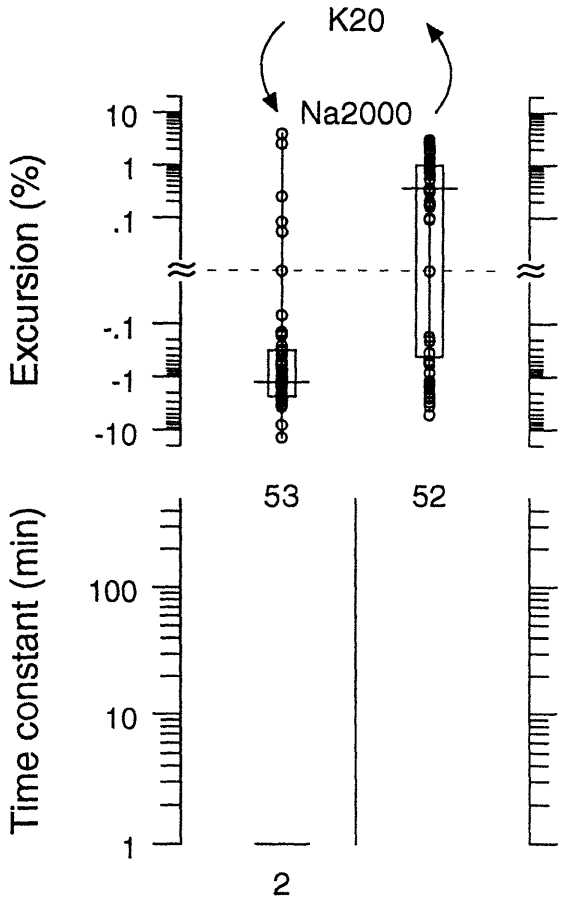

Figure 3.4: Parameters of exponential functions fit to measurements of bead height during transitions between artificial endolymph (K20) and artificial perilymph (Na2000).
This figure shows results for both transitions, indicated by the direction of the arrows at the top of the columns. Circles in the top panel indicate excursions (as a percentage of overall thickness), which are defined as the difference between the value of the fitted exponential at the end of the perfusion interval and the value at the beginning of the interval. Circles in the bottom panel indicate time constants of the exponential fits. Box plots indicate the medians and the interquartile ranges. The number of data points is indicated beneath each set of data. Because estimates of time constants are poor when excursions are small compared to measurement noise, the number of reported time constants is usually smaller than the corresponding number of excursions.

Solution Transition	Median z-excursion (μm)	Median z-excursion (% overall thickness)
K20-Na2000	-0.227	-1.252
Na2000-K20	0.0825	0.3625

Table 3.1: Table of median z-axis excursions in microns and percentage of overall thickness during transitions between artificial endolymph (K20) and artificial perilymph (Na2000).

Results are pooled for 2 preparations, during which 9 such transitions took place. Although there is scatter, there are some clear trends visible in the medians and the interquartile ranges. For the K20-Na2000 transition, there is a small median shrinking of -1.25% (-0.227 μm), and for the Na2000-K20 transition there is a small median swelling of 0.36% (0.0825 μm). Because the median swelling and shrinking responses are of comparable magnitude, reversibility of the responses is strongly suggested.

Despite the scatter, these results are statistically significant because the interquartile ranges are largely non-overlapping. Time constants that were computed for these exchanges were deemed unreliable due to the small magnitude of the responses and are not included here.

3.2 Effects of exchanging sodium and potassium as predominant cation

Figure 3.5 and Table 3.2 summarize the effects of exchanges between solutions that were identical except for predominant cation (either K^+ or Na^+). Four such exchanges with different constant calcium concentrations were studied: (1) zero added calcium, (2) 20 μM added calcium, (3) 2000 μM added calcium, and (4) EGTA-buffered zero calcium.

Both Figure 3.5 and Table 3.2 show that the greatest median z-excursions of 3.51% (0.632 μm) and -2.81% (-0.521 μm) took place when sodium-potassium exchanges were performed while holding the added calcium concentration at 20 μM. These results are followed closely by values from 0 μM added calcium: 1.87% (0.408 μm), and -1.92% (-0.509 μm).

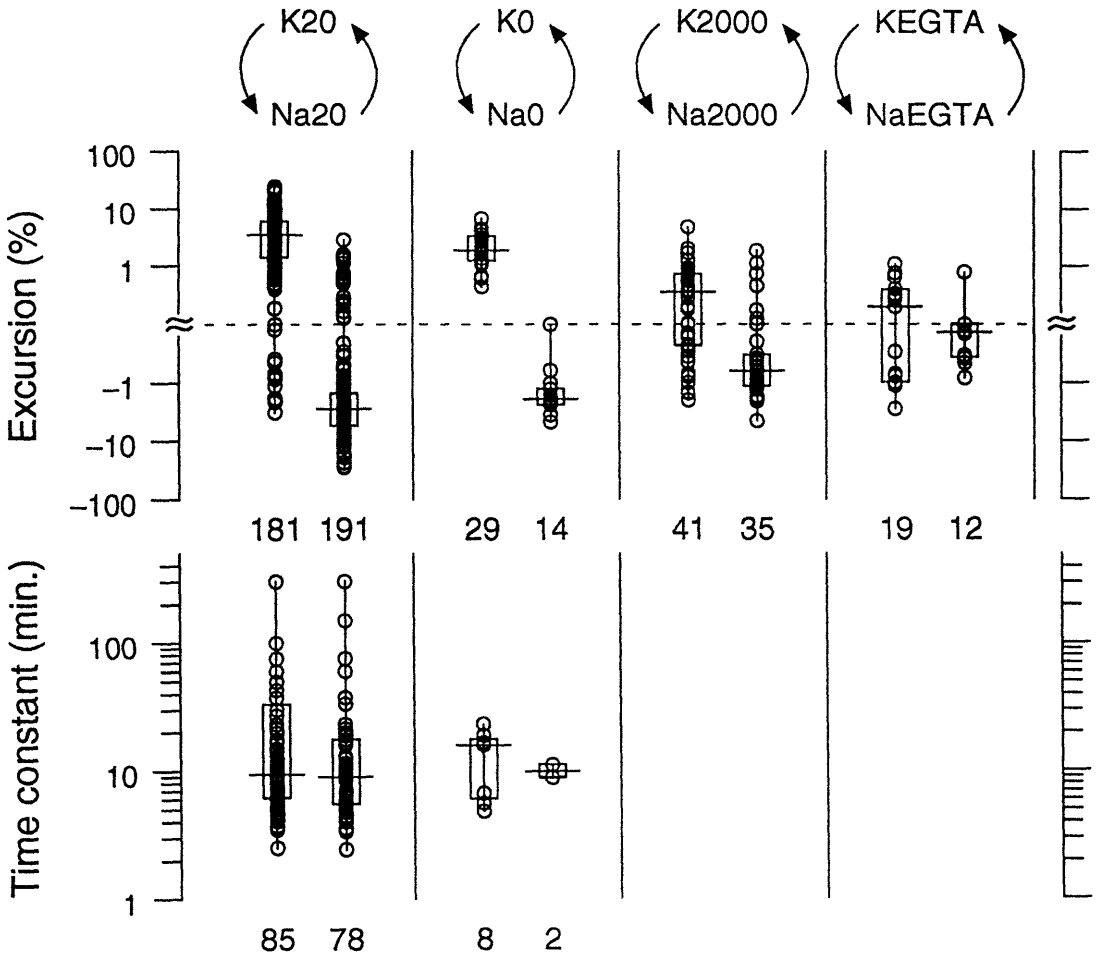

Figure 3.5: Parameters of exponential functions fit to bead heights measurements during transitions between high-Na^+ and high-K^+ solutions.
This figure shows results for 8 different transitions, indicated by the direction of the arrows at the top of the columns. The method for displaying these results is described in Figure 3.1.

Solution Transition	**Median z-excursion (μm)**	**Median z-excursion (% overall thickness)**
KEGTA-NaEGTA	0.135	0.199
K0-Na0	0.408	1.87
K20-Na20	0.632	3.508
K2000-Na2000	0.117	0.351
NaEGTA-KEGTA	-0.0805	-0.1365
Na0-K0	-0.509	-1.924
Na20-K20	-0.521	-2.809
Na2000-K2000	-0.231	-0.639

Table 3.2: Table of median z-axis excursions in micrometers and percentage of overall thickness for predominant cation exchanges with calcium concentrations held constant.

In both EGTA-buffered and very high (2000 μM) calcium concentrations, substituting Na^+ for K^+ gave rise to small swelling responses close to our noise threshold. For an EGTA-buffered 0 μM calcium solution, z-excursions were 0.199% (0.135 μm), and -0.137% (-0.081 μm). For 2000 μM added calcium, z-excursions were determined to be: 0.351% (0.117 μm), and -0.639% (-0.231 μm).

Both Figure 3.5 and Table 3.2 show that the greatest median z-excursions of 3.51% (0.632 μm) and -2.81% (-0.521 μm) took place when sodium-potassium exchanges were performed while holding the added calcium concentration at 20 μM. These results are followed closely by values from 0 μM added calcium: 1.87% (0.408 μm), and -1.92% (-0.509 μm).

In both EGTA-buffered and very high (2000 μM) calcium concentrations, substituting Na^+ for K^+ gave rise to small swelling responses close to our noise threshold. For an EGTA-buffered 0 μM calcium solution, z-excursions were 0.199% (0.135 μm), and -0.137% (-0.081 μm). For 2000 μM added calcium, z-excursions were determined to be: 0.351% (0.117 μm), and -0.639% (-0.231 μm).

Reliable time constants were determined only for the K20-Na20, Na20-K20, K0-Na0 and Na0-K0 transitions, because response magnitudes were generally too small in the other cases. The time constant medians range from 9.4 to 15.8 minutes.

From the median responses and their associated interquartile ranges, it appears that sodium-potassium induced swelling and shrinking at different calcium concentrations is a reversible phenomenon.

3.3 Effects of altering calcium concentration

Figure 3.6 and Table 3.3 summarize all z-axis excursions in percentage of overall thickness and in micrometers over all intervals where calcium concentration was altered with potassium as the predominant cation.

Both Figure 3.6 and Table 3.3 indicate that altering the calcium concentration in the artificial lymphs produces osmotic responses in the tectorial membrane like those in exchanges of solutions with different predominant cation.

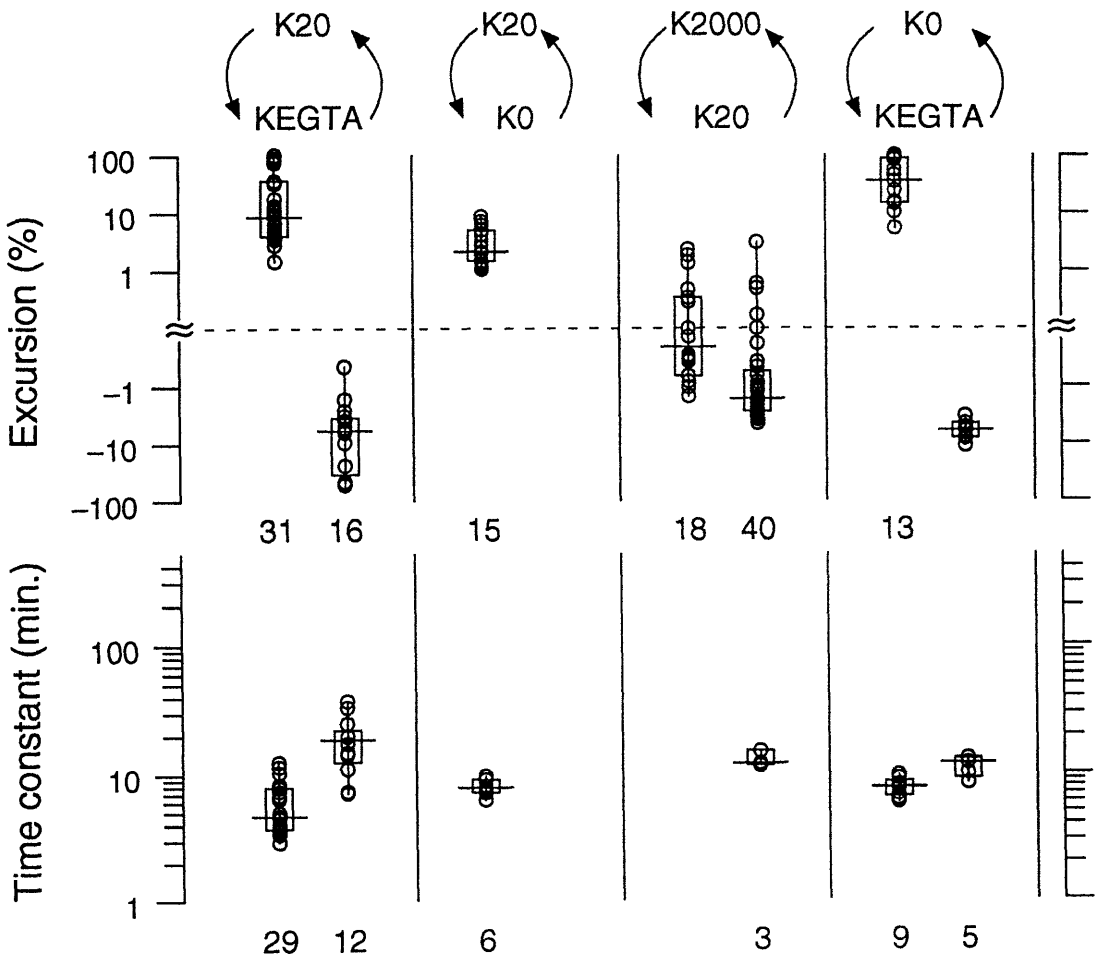

Figure 3.6: Parameters of exponential functions fit to measurements of bead heights during transitions between low Ca^{2+} and high-Ca^{2+} solutions and EGTA solutions, with K^+ as the predominant cation.
This figure shows results for 8 different transitions, indicated by the direction of the arrows at the top of the columns. The method for displaying these results is described in Figure 3.1.

Solution Transition	**Median z-excursion (μm)**	**Median z-excursion (% overall thickness)**
KEGTA-K0	-0.735	-6.057
KEGTA-K20	-3.513	-5.8635
K0-K20		
K20-K2000	-0.383	-1.6715
K0-KEGTA	6.811	35.625
K20-KEGTA	3.873	8.525
K20-K0	0.294	2.133
K2000-K20	-0.037	-0.2145

Table 3.3: Table of median z-axis excursions in micrometers and percentage of overall thickness for calcium concentration changes with K^+ held constant as the predominant cation.

Upon addition of calcium, systematic shrinking of the tectorial membrane was observed. The largest median z-excursions of -6.06% (-0.735 μm) and -5.86% (-3.51 μm) occurred with KEGTA-K0 and KEGTA-K20 intervals, where calcium concentration increases from an EGTA-buffered 0 μM to either zero added calcium or 20 μM added calcium. When increasing to even higher calcium concentrations, as is the case with a K20-K2000 transition, further shrinking was observed, but at a smaller magnitude of -1.67% (-0.383 μm).

Systematic swelling of the tectorial membrane was observed with the removal of calcium. The largest observed median z-excursion was 35.63% (6.811 μm) and occurred with K0-KEGTA exchanges. Other decreases in calcium concentration also resulted in swelling responses, but with progressively smaller magnitudes as higher starting calcium concentrations were used: K20-KEGTA, K20-K0. The sole exception to this behavior was seen in the K2000-K20 transition, which had a very slight shrinking median response of -0.21% (-0.037 μm), a value that falls into the range of our measurement noise.

Time constant estimates were determined for all changes in calcium concentration in potassium except for K0-K20 and K2000-K20. The medians for time constants range from 4.4 minutes to 18.8 minutes with the faster time constants associated with transitions to KEGTA and calcium removal from solution.

From the interquartile ranges and medians in Figure 3.7, it appears that the responses to calcium concentration changes in potassium are at least partially reversible.

Figure 3.7 and Table 3.4 summarize all z-axis excursions in percentage of overall thickness and micrometers over all intervals where calcium concentration was changed with sodium as the predominant cation.

Upon addition of calcium, the same systematic shrinking response seen with potassium as the predominant cation occurred. The largest median z-excursion of -4.98% (-2.601 μm) was associated with the KEGTA-K0 and KEGTA-K20 intervals, where calcium concentration changes from an EGTA-buffered 0 μM to 20 μM added calcium. Other calcium concentration changes resulted in shrinking responses that were less than half the magnitude of the maximum response.

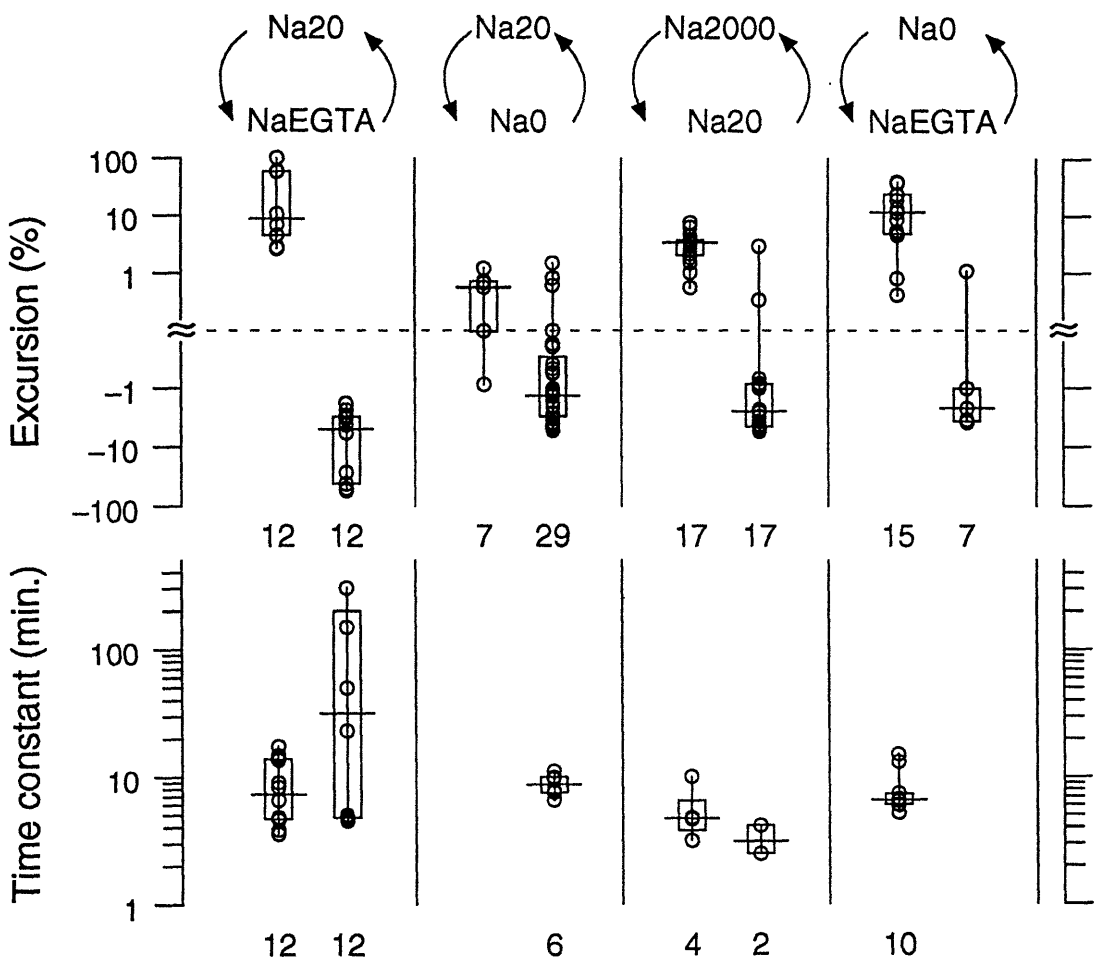

Figure 3.7: Parameters of exponential functions fit to measurements of bead heights during transitions between low Ca^{2+} and high-Ca^{2+} solutions and EGTA solutions, with Na^+ as the predominant cation.
This figure shows results for 8 different transitions, indicated by the direction of the arrows at the top of the columns. The method for displaying these results is described in Figure 3.1.

Solution Transition	**Median z-excursion (μm)**	**Median z-excursion (% overall thickness)**
NaEGTA-Na0	-0.305	-2.236
NaEGTA-Na20	-2.605	-4.977
Na0-Na20	-0.277	-1.379
Na20-Na2000	-0.376	-2.535
Na0-NaEGTA	2.939	11.527
Na20-NaEGTA	3.996	8.763
Na20-Na0	0.143	0.567
Na2000-Na20	0.538	3.459

Table 3.4: Table of median z-axis excursions in micrometers and percentage of overall thickness for calcium concentration changes with Na^+ held constant as the predominant cation.

Systematic swelling of the tectorial membrane was also observed with the removal of calcium. The largest median z-excursion in percentage was 11.53% (2.939 μm) associated with Na0-NaEGTA exchanges. In micrometers, the largest median z-excursion was 3.996 μm (8.76%) associated with Na20-NaEGTA exchanges. Other non-EGTA associated exchanges that decreased calcium concentration resulted in much smaller swelling responses.

Time constant estimates were determined for all changes in calcium concentration in sodium except for Na20-Na0 and NaEGTA-Na0. The medians for time constants range from 3.2 minutes to 34 minutes with the faster time constants associated with transitions to the higher calcium concentrations and transitions to EGTA lymphs. The slowest time constant of 34 minutes was associated with the NaEGTA-Na20 transition, where a small amount of calcium was added with the calcium chelator EGTA present.

From the median responses and their associated interquartile ranges, it appears that calcium-induced osmotic responses with Na^+ as the predominant cation are reversible phenomena.

3.4 Swelling and shrinking in the x-y plane

Shrinking and swelling was apparent not only as changes in z-axis positions of beads, but also as changes in the apparent area of video images (i.e. in the x-y plane).

We characterized these changes in the x-y plane by generating outline drawings (Figure 3.8) and computing the areas enclosed by the outlines [5]. Areas were computed for 22 K20-Na20 transitions in our dataset.

Outlines were prepared from images taken at the end of intervals to ensure that final states and not transients were captured.

Swelling responses produced area changes ranging from +5.5% to +11.2%, and shrinking responses produced area changes ranging from -4.4% to -11.6%.

If area changes are assumed to result from radially symmetric expansion and contraction, changes in the x and y directions can be estimated as the square root of the change in area. For swelling, x and y changes range from +2.7% to +5.5% and for shrinking, x and y changes range from -2.2% to -5.6%.

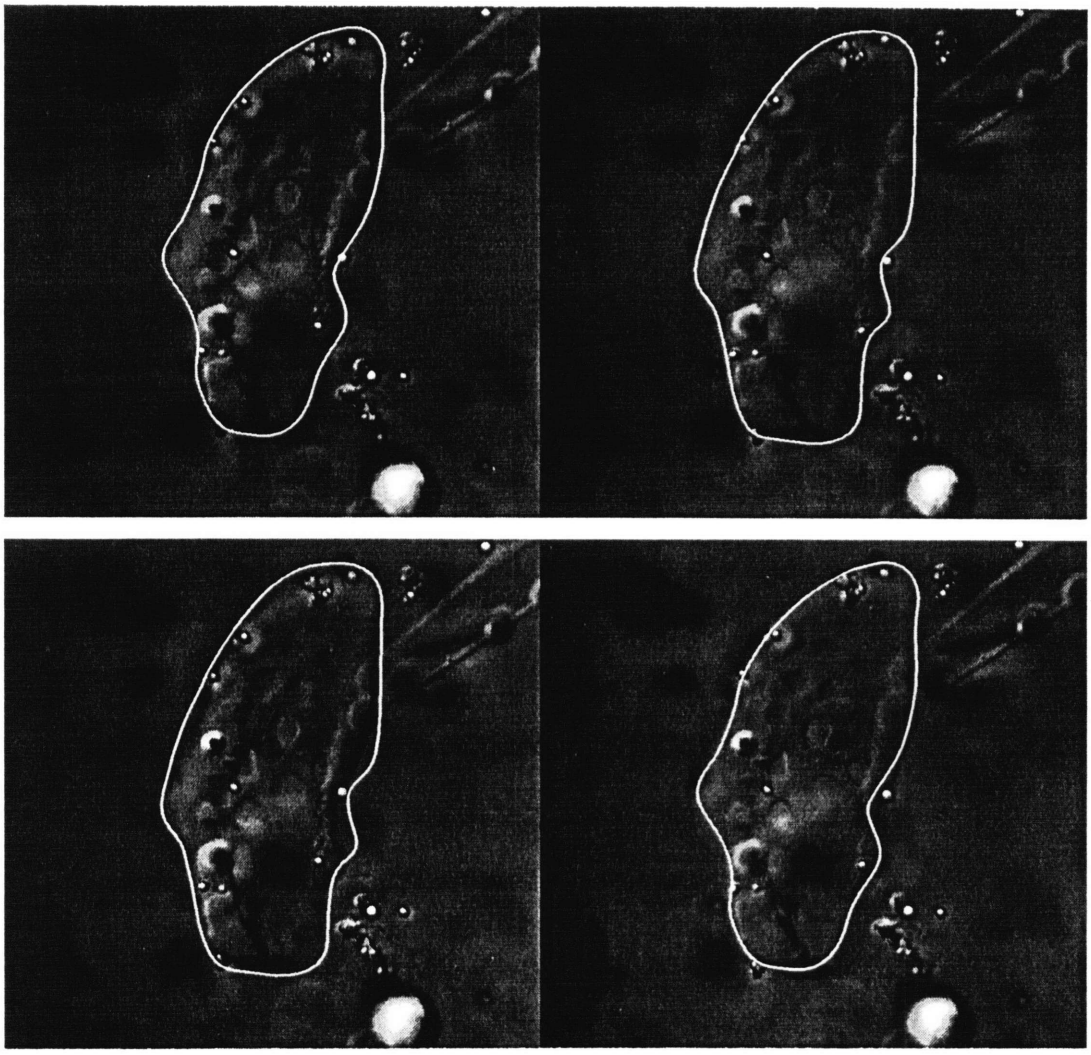

Figure 3.8: Tectorial membrane images and associated area tracings.
The top pair of images illustrates the tectorial membrane in K20 (left) and Na20 (right). The white lines are manually generated outlines following the perimeter of the tectorial membranes as seen by the author. The bottom pair of images is identical to the first, except that the outlines have been exchanged for comparison.

If we compare our z-excursions in percentage for the K20-Na20 (3.51%) and Na20-K20 (-2.81%) exchanges to our estimated x and y changes, it becomes apparent that all of the values are of almost identical magnitudes.

This indicates that changes in the z-axis are comparable to changes in the x and y axes. Further support for such a correlation is lent by Figure 3.9.

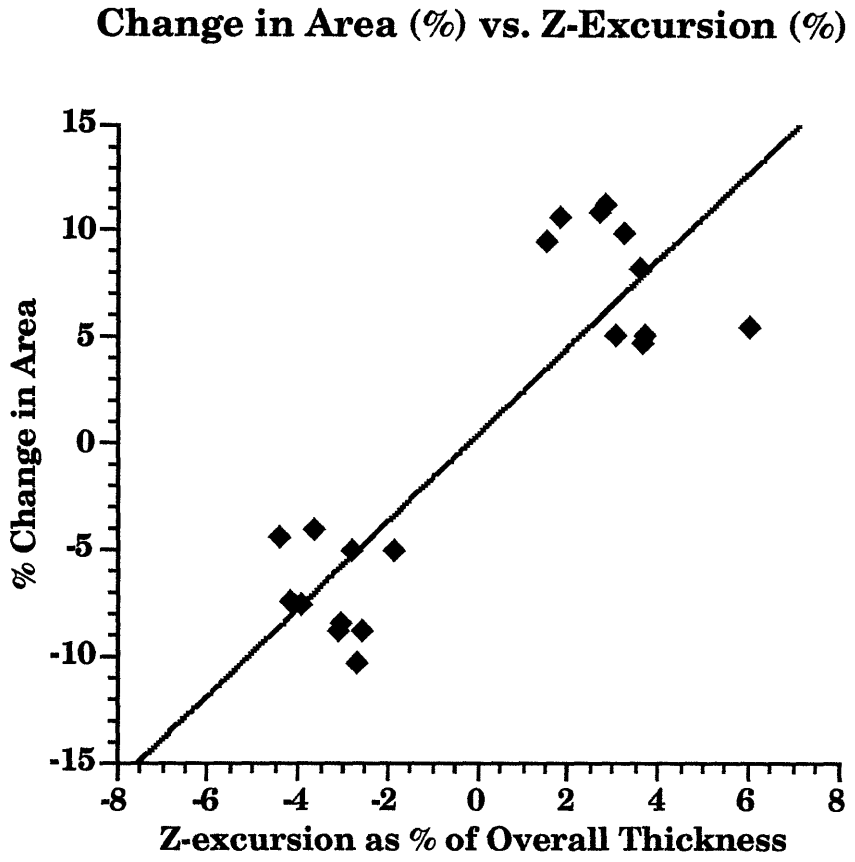

Figure 3.9: Change in area as a percentage of overall area versus z-axis excursion as a percentage of overall thickness.
Each point represents a K20-Na20 or Na20-K20 transition and the associated changes in area and thickness. To convert area changes into estimates of one-dimensional changes along the x or y axes, the square root of the area change should be computed.

These results suggest that the tectorial membrane experiences isotropic expansion and contraction. Therefore, excursions along the z-axis capture the same primary information as area changes in the x-y plane and can be considered reflective of swelling and shrinking behavior of the tectorial membrane in these experiments.

3.5 Additional observations concerning osmotic responses

Several qualitative observations can be made concerning the changes in the dimensions of tectorial membrane.

During the course of an experiment, it appeared that the holes in the tectorial membrane would open and close as part of the swelling-shrinking process. This behavior is consistent with the outward normal swelling description.

Another potentially important observation is the apparent deterioration of the tectorial membrane's surface microstructure as experimental run time progressed. Small surface striations that were visible at the onset of an experiment would become less apparent and generally disappear completely after 24 hours after dissection. However, while these striations were visible, it was observed that perfusates that induced shrinking in the tectorial membrane enhanced the definition of any external microstructural features and the opposite case was also found to be true. The most dramatic examples of this behavior occurred with perfusates that induced significant swelling, especially the EGTA lymphs, which resulted in the disappearance of external features previously visible in a unswelled state as depicted in Figure 3.10.

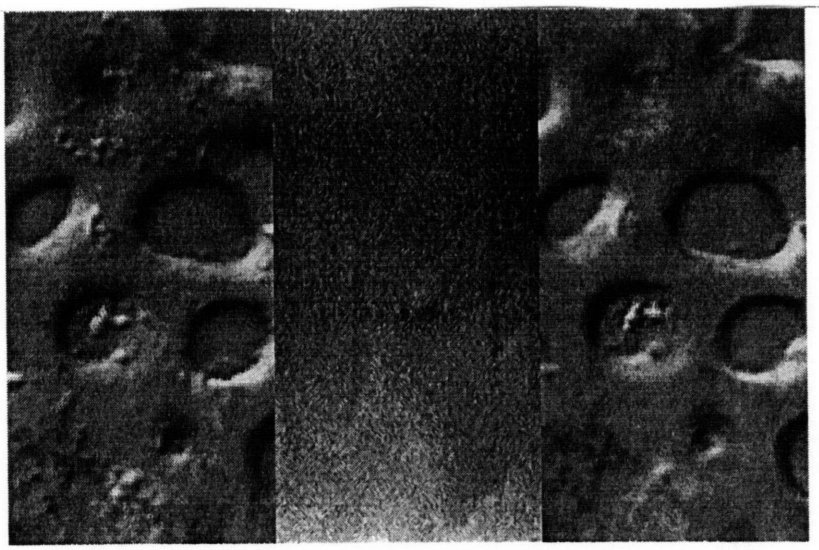

Figure 3.10: Sequence of images taken of the tectorial membrane during different perfusion intervals.
This sequence of pictures illustrates the dramatic change in surface features as the tectorial membrane is exposed to intervals of K20, KEGTA, and K20 sequentially. There is a general disappearance of surface features, such as texture and striations. Also, note the disappearance or closure of hair bundle holes.

3.6 Observations concerning the morphology of the tectorial membrane

In the process of manipulating and isolating a tectorial membrane, several observations concerning the morphology of the tectorial membrane were made.

In situ, the tectorial membrane rests on and surrounds short stereociliary bundles of the basilar papilla. The top of the tectorial membrane exhibits a number of well-defined small circular apertures that increase in diameter to match the size of stereociliary bundles as the basilar papilla is approached. A tectorial membrane *in situ* is shown in Figure 3.11.

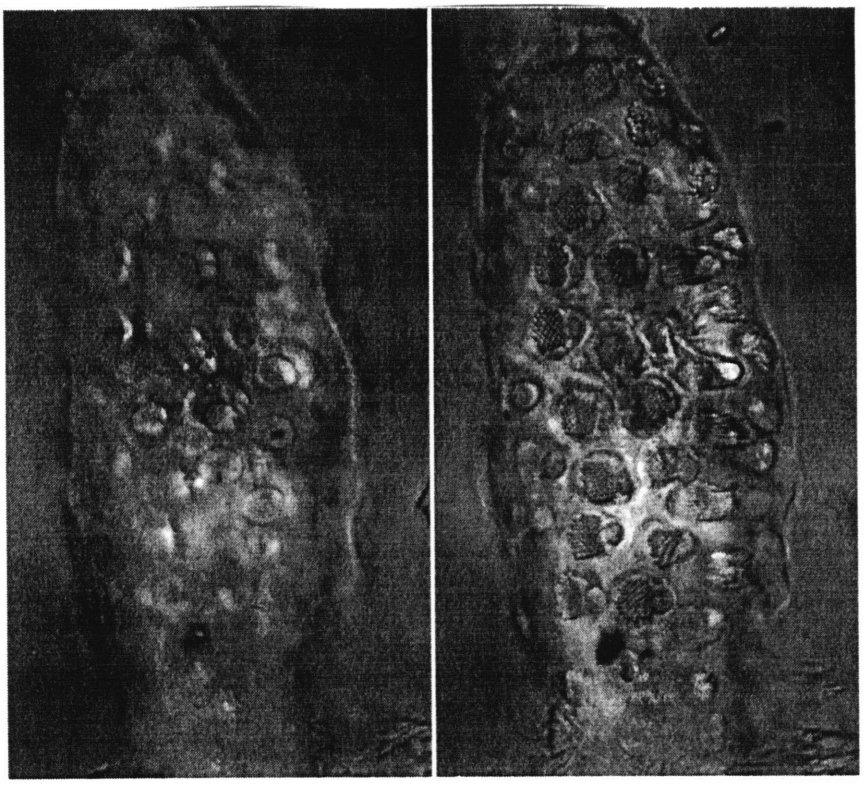

Figure 3.11: Images of an *in-situ* tectorial membrane surrounding and overlying hair bundles on tectorial region of the basilar papilla. These pictures illustrate the natural condition of the tectorial membrane. In the left panel, the top surface of the tectorial membrane is illustrated. Note the periphery of the tectorial membrane and the presence of circular apertures of different sizes. The right panel illustrates the same region, but at the level where hair bundles tips are visible. The tips of hair bundles appear as hexagonally packed dots in circular apertures of the tectorial membrane. Also visible along the right side of the image are several hair bundles in profile, with the tectorial membrane overlying it. At the bottom of both images, tall stereocilia from the free-standing region can be seen.

There does not appear to be a one-to-one relationship of apertures in the top to the total number of stereociliary bundles in the tectorial region, which suggests that a number of these holes surrounding stereociliary bundles close completely as they reach the top of the tectorial membrane.

At their widest, these holes are just large enough to allow the passage of one stereociliary bundle through, although it is uncertain whether the bundles are in actual contact with the tectorial membrane.

When separated from the basiliar papilla, it is clear that the tectorial membrane conformed to and retains the general convex shape of the tectorial region of the basilar papilla as seen in Figure 3.12.

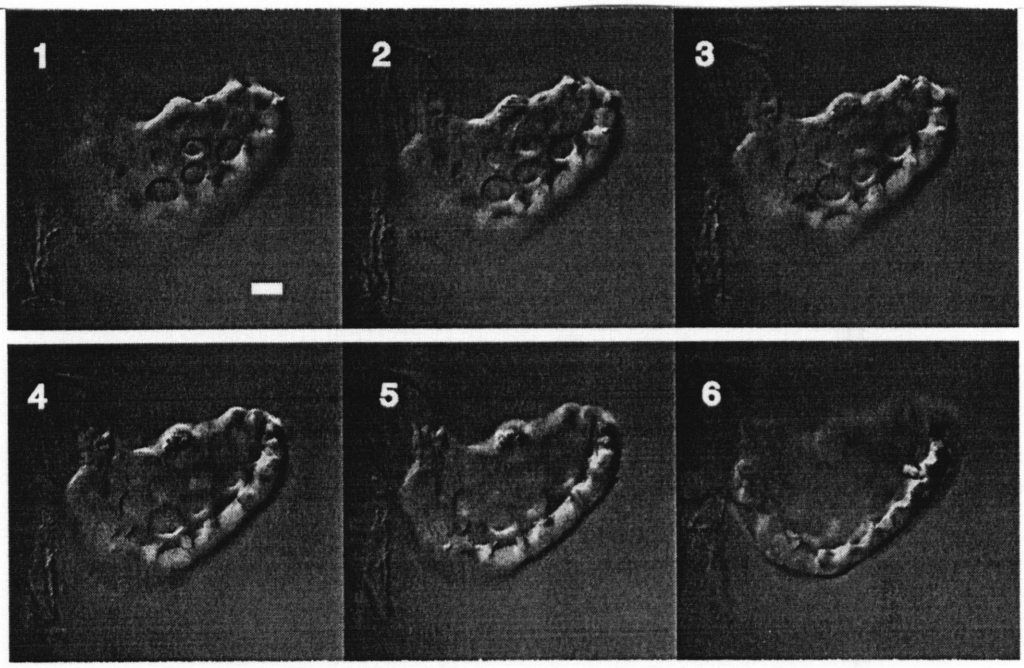

Figure 3.12: Sequence of optically sectioned images taken of a free-floating tectorial membrane immediately after being separated from the basilar papilla. The images begin at the rear surface of the tectorial membrane (upper left, #1), and progress forward from left to right and line by line until the leading edge of the tectorial membrane (bottom right, #6) is reached. The length of the scale bar in panel #1 is equivalent to 10 micrometers. Features not clearly in focus are out of the plane being displayed. This sequence of images illustrates the naturally concave shape of the tectorial membrane. Note that some holes go completely through the tectorial membrane, whereas others, especially those along the edge do not.

When isolated, the tectorial membrane exhibits the same physical characteristics as it does *in situ*. The circular apertures are very apparent, as are their changes in diameter upon optical sectioning. Also apparent in some

preparations, like that illustrated in Figure 3.13, are kinociliary bulbs, appearing as isolated spots along the edges of some apertures. This suggests that a portion of stereociliary bundles is physically linked to the tectorial plate.

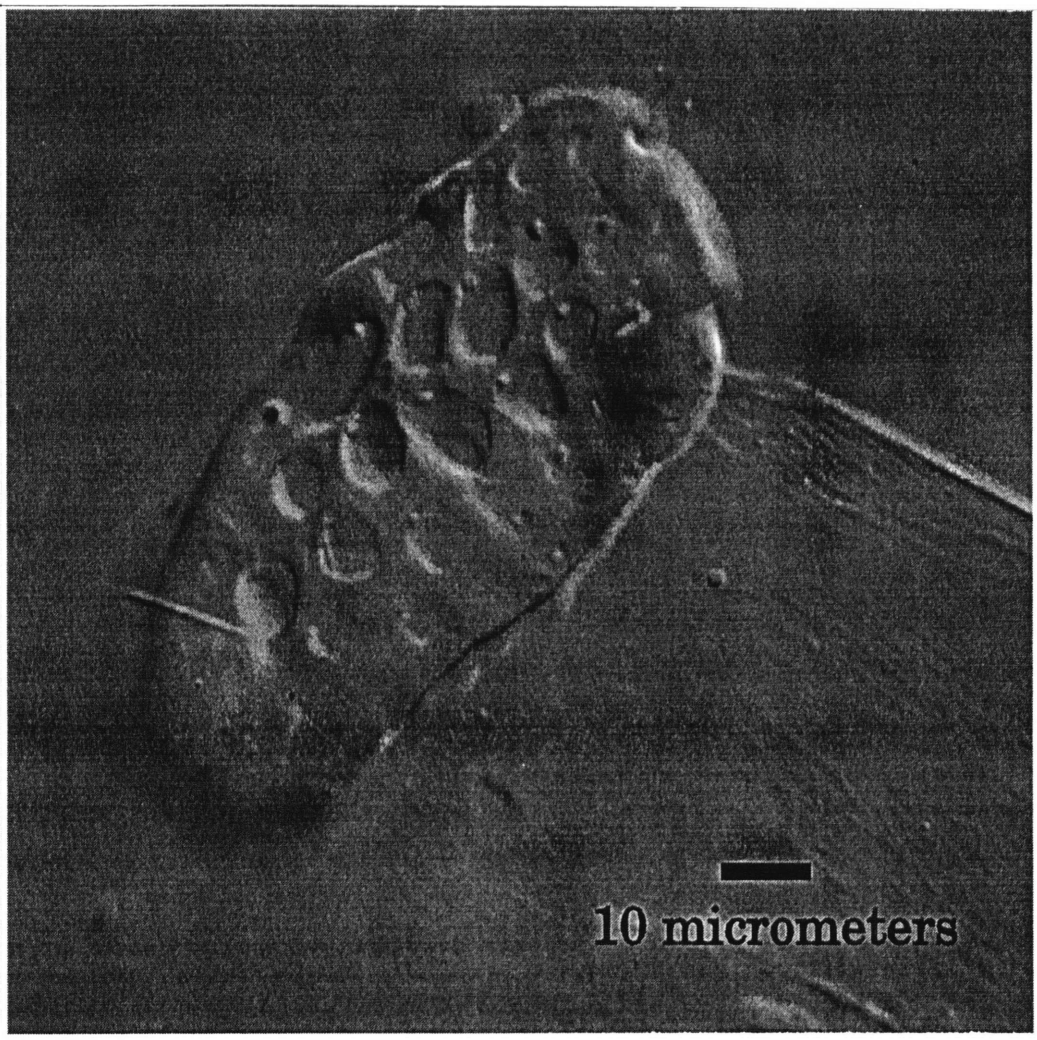

Figure 3.13: Image of an isolated tectorial membrane affixed to Cell-Tak.
This picture illustrates the condition of the tectorial membrane after isolation and being affixed to the cellular adhesive Cell-Tak. Note the presence of a number of holes protruding through the tectorial membrane, and the presence of what appear to be kinociliary bulbs near the edges of these holes. Also note the tectorial membrane veil leading away from the tectorial membrane and its distinct striated structure.

From both *in situ* and isolated tectorial membranes, the thickness of the tectorial plate was found to be typically between 30-35 μm, whereas the veil portion is less than 1 μm thick.

The veil portion of the tectorial membrane is very different from the thick tectorial plate on the basilar papilla. In addition to being much thinner, it possesses no holes and shows delicate striations lengthwise in the region where it bridges between the tectorial plate (see Figure 1.1) and the neural limbus. In the region where it is anchored to the neural limbus, it exhibits hexagonal cellular imprints.

3.7 Summary of Results

- Small, reversible shrinking occurred in the tectorial membrane when artificial endolymph (K20) was replaced with artificial perilymph (Na2000).
- Small, reversible swelling occurred when the predominant cation was changed to from potassium to sodium.
- Larger, partially reversible swelling and shrinking was observed by altering calcium concentration, especially with calcium removal by EGTA-buffered solutions.
- Magnitude of swelling and shrinking responses did not change after 24 hours.
- Surface microstructural features became less apparent over time and in situations where the tectorial membrane had swelled.
- Holes would appear to close and open uniformly with swelling and shrinking consistent with an outward normal swelling-shrinking pattern.
- The *in situ* and isolated tectorial membranes exhibit holes for hair bundles and typical thickness range from 30-35 μm.
- A one-to-one relationship of holes passing completely through the *in situ* and isolated tectorial membrane to hair bundles does not exist.
- Kinociliary bulbs were found on the tectorial membrane.
- The veil portion of the tectorial membrane is approximately 1 μm thick, and possesses hexagonal cellular imprints where it is in contact with the neural limbus and striations elsewhere.

Chapter 4: Discussion

4.1 Gel models

As discussed in the introduction, the composition of the tectorial membrane has been determined to resemble that of a polyelectrolyte gel. To achieve a state of overall equilibrium, a polyelectrolyte gel must maintain osmotic, mechanical, and electrochemical equilibrium in addition to maintaining macroscopic charge neutrality [7, 17, 21, 27].

Gel models have been used to accurately describe the physicochemical behavior of a number of other naturally occurring tissues, including the avian and mammalian tectorial membranes [4, 7, 22]. In this section, we discuss our results for the alligator lizard in terms of gel mechanisms.

4.1.1 Osmotic responses to isosmotic solution changes

A number of osmotic responses were observed in the alligator lizard tectorial membrane in solutions of the same osmolarity and ionic strength, but different ionic compositions.

Similar observations made in avian and mammalian tectorial membrane were conjectured to be the result of differential binding of cations to the tectorial membrane [4, 22].

4.1.2 Effect of exchanging sodium and potassium as predominant cation

Exchanging sodium for potassium as the predominant cation systematically resulted in a swelling response. This behavior was consistent, regardless of the calcium concentration. If we interpret the swelling as a purely osmotic response due to a change in fixed charges on the tectorial membrane, then the increase in sodium concentration and the corresponding decrease in potassium concentration must result in a net increase in the fixed charge on the tectorial membrane. This net increase in fixed charge would be responsible for increased ion swelling pressure and the resultant swelling [4].

4.1.3 Effect of calcium concentration changes

Indicate that increasing the calcium concentration by a small amount (2 mM) resulted in shrinkage of comparable or greater magnitude than that associated with predominant cation exchange. Reducing calcium concentration by returning to the original low calcium solution resulted in a swelling response of the same magnitude. Addition of the calcium chelator EGTA to remove trace levels of calcium from the bath solution resulted in extremely large swelling responses. From our limited set of time constant results, the addition of EGTA also resulted in the most rapid changes observed. The simple addition of calcium to a non-EGTA solution also resulted in rapid responses.

These results are consistent with a hypothesis that a calcium binding site exists on a tectorial membrane macromolecule [4]. Consequentially, the addition of calcium would increase the amount of bound calcium in the tectorial membrane, thereby reducing the negative fixed charge and resulting in the observed dehydration. The opposite reaction, hydration, would be expected occur if a calcium-chelator such as EGTA were introduced into solutions.

4.1.4 Effect of substituting artificial perilymph for artificial endolymph

Exchanging artificial perilymph for artificial endolymph resulted in a minute shrinkage. Results can be understood as the small amount of calcium in artificial perilymph offsetting the swelling that would be expected for a high-sodium solution.

This is of physiological interest because the inner ear is known to actively regulate the concentration of these ions. Acoustic overstimulation and various pathological conditions are thought to alter the concentrations of these ions, possibly by the mixing of endolymph and perilymph [5]. Our results show that changes in concentration are likely to have dramatic effects on the tectorial membrane.

4.1.5 Reversibility

Exposing the tectorial membrane to ionic environments of different composition resulted in swelling and shrinking that was always at least partially reversible, and in some cases fully reversible. The nature of the reversibility was

dependent only upon the ionic environment and not upon the duration of exposure. Swelling and shrinking associated with changes in predominant cation (Na^+ and K^+) appear to be completely reversible because their median % z-excursions are almost identical. However, if we use the same criterion to examine the median % z-excursions for the calcium-induced changes, they are less convincing in demonstrating full reversibility. This deviates from previously seen behavior in the avian tectorial membrane, but is consistent with behavior seen in the mammalian tectorial membrane [4, 22].

A number of simple mechanisms could be responsible for the nature of this irreversibility. The partial irreversibility seen with calcium concentration changes could be the result of the aforementioned extreme sensitivity to even slight variations in calcium concentration. Another possibility is a chemical effect whereby altering Ca^{2+} concentration irreversibly alters the biochemical structure of the tectorial membrane.

A non-chemical explanation of irreversibility relies on the mechanical disruption of the microstructure of the tectorial membrane. However, a lack of observations regarding the ultrastructure of the alligator lizard tectorial membrane only allows us to speculate that swelling and shrinking beyond a certain magnitude disrupts a natural mesh-like ultrastructure and irrevocably changes the tectorial membrane much like in the case of the avian tectorial membrane [4]. Unfortunately, this explanation is further complicated by the fact that some of the largest swelling and shrinking responses induced by changes in predominant cation is fully reversible. In light of this fact, it seems that a chemical effect is the most likely to be responsible for any irreversibility seen in these experiments, but further study directly addressing this problem is required to definitively identify if a source of irreversibility exists.

4.2 Comparison with previous measurements

Comparison with other tectorial membrane studies can be considered in two separate groups. The early studies on the effect of ionic environment were performed *in situ* and provided conflicting results. More recent studies have examined isolated tectorial membranes, a technique which has removed many potential sources of ambiguity.

4.2.1 Early studies

The early observations of the effect of ionic composition on the tectorial membrane were all performed on the mammalian cochleas of mice, guinea pigs, and rabbits [13, 14, 18, 23, 24].

Results from the most systematic of these studies indicated that the tectorial membrane shrinks irreversibly (-20% change in thickness), when the bathing solutions is changed from artificial endolymph to artificial perilymph [13, 14]. Also, the tectorial membrane was reported to swell greatly (> 80% change in thickness) if the divalent chelator EDTA was added to the bathing solution and to shrink if Ca^{2+} was added to the bathing solution.

Other studies using similar preparations to that used by Kronester-Frei, reported that altering Ca^{2+} concentration between 20 μM and 2000 μM in artificial endolymph solutions had no effect upon the tectorial membrane [18]. It has also been reported that the isolated mouse tectorial membrane shrinks in high-sodium solutions; unfortunately, Ca^{2+} concentrations were not reported [23].

Our results differ significantly from results reported in these early studies of the tectorial membrane; however, this could be the result of the many differences in methodologies and solution characteristics.

4.2.2 Recent studies

Recent studies of the isolated chick and mouse tectorial membrane indicate that a certain amount of physicochemical consistency exists among vertebrate tectorial membranes. [4, 22]

Substituting artificial perilymph for artificial endolymph produced a small, reversible shrinking for all three species. The median excursions were -15% in the chick, -1.3% in the mouse, and -1.25% in alligator lizard. These values are considered small for each species when compared to other osmotic responses seen in the studies. Time constants were basically similar in all three species, all three being approximately 10 minutes. The exception to this was swelling in the chick (~40 minutes) upon return to artificial endolymph.

All three species' tectorial membranes were observed to swell in solutions with sodium as the predominant cation. For high sodium solutions, the added calcium concentration in which maximum swelling occurred was 20 μM for the

alligator lizard, but 0 μM for the chick and the mouse. However, a large response was also seen for the alligator lizard at 0 μM added calcium. Common to all three species are reduced magnitude swelling responses at 2000 μM added calcium and in the EGTA-buffered solutions. However, there was variation in the time constants for potassium-sodium exchanges in all three species. For chick, time constants ranged from 2-20 minutes; for mouse, 9-43 minutes, and for alligator lizard, 9-18 minutes.

Altering the calcium concentration also induced similar responses from all three species' tectorial membranes. Swelling was seen as calcium was removed from the bath solutions. In addition, the calcium chelator EGTA was consistent in inducing the largest overall swelling responses for each species.

The calcium associated time constants that were deemed reliable for the alligator lizard tectorial membrane are also consistent with those reported in the avian and mammalian tectorial membrane. In the chick and mouse, rapid responses with were seen when calcium was added (time constants < 10 minutes), or when the calcium-chelator EGTA was introduced (time constants < 5 minutes). Slower responses were seen when the calcium concentration of the bath was lowered (time constants 10-100 minutes). The time constants associated with calcium concentration changes suggest that a calcium binding site exists for chick and mammal -- unfortunately, a lack of time constants for calcium effects in alligator lizard precludes the possibility of generalizing to include our results. However, the observed sensitivity to the alligator lizard tectorial membrane to the calcium chelator EGTA lends support to the potential of a calcium binding site [4].

Interspecies differences become apparent when one considers secondary aspects of swelling and shrinking responses, such as magnitude and reversibility. In general, the chick was observed to have extremely large responses, with median % excursions greater than 10% in most cases, whereas the responses of the alligator lizard and the mouse were significantly smaller, with median % excursions typically less than 10%.

Irreversibility to long-duration swelling responses in high sodium concentrations was seen in the chick, a feature not seen in either the alligator lizard or the mouse -- suggesting a fundamental difference in biochemical structure or in the mechanical microstructure.

4.3 Implications of the results

The results have implications for understanding the micromechanics of the inner ear as well as having physiological implications.

4.3.1 Micromechanical implications

The classic models of the inner ear depict the tectorial membrane as a rigid body, capable of only pivoting, translating, and transmitting forces in a lever-like system without introducing any form of dynamics.

Our results combined with those of others suggest that modeling the tectorial membrane as a gel is the appropriate approach to understanding its mechanical properties. Its distributed properties are capable of introducing dynamic behavior to a system and a thorough understanding from a gel perspective may provide an acceptable explanation of inner auditory system functions.

4.3.2 Physiological implications

The osmotic responses observed in this study have physiological implications by themselves. The extreme close proximity of endolymph and perilymph in the inner ear makes it possible for these two radically different fluids to mix in random proportions. This fluid mixing allegedly occurs in some forms of acoustic trauma and even some pathological conditions. Our results suggest that the mixing of endolymph with perilymph would have a definite effect upon the state of the tectorial membrane and this in turn would affect its ability to fulfill its mechanical role in transducing an acoustic stimulus.

A second physiological implication from our results centers around the tectorial membrane's extreme sensitivity to calcium concentration. This observation when combined with the fact that calcium is a highly regulated species in inner ear fluids makes it plausible that it may be part of a natural, long term adaptive mechanism for the tectorial membrane.

References

[1] Bosher, S.K. and Warren, R.L. (1978). **Very low calcium content of cochlear endolymph, an extracellular fluid**. *Nature*, 273:377-378.

[2] Dana, K.J. (1992). **Three-dimensional Reconstruction of the Tectorial Membrane: An Image Processing Method using Nomarski Differential Interference Contrast Microscopy**. *M.I.T. Department of Electrical Engineering and Computer Science, Masters Thesis.*

[3] Fan, L.M. (1991). ***In vitro* swelling of the alligator lizard cochlear duct in artificial endolymph**. *M.I.T. Department of Electrical Engineering and Computer Science, Bachelors Thesis.*

[4] Freeman, D.M., Cotanche, D.A., Ehsani, F., Weiss, T.F. (1994). **The osmotic response of the isolated tectorial membrane of the chick to isosmotic solutions: Effect of Na^+, K^+ and Ca^{2+} concentration**. (Submitted for publication).

[5] Freeman, D.M., Hendrix, D.H., Shah, D., Fan, L.F., and Weiss, T.F. (1993). **Effect of lymph composition on an *in vitro* preparation of the alligator lizard cochlea**. *Hearing Research*, 65:83-98.

[6] Frishkopf, L.S. and DeRosier, D.J. (1983). **Mechanical tuning of free-standing stereociliary bundles and frequency analysis in the alligator lizard cochlea**. *Hearing Research*, 12:393-404.

[7] Grodzinsky, A.J. (1983). **Electromechanical and physicochemical properties of connective tissue**. *CRC Crit. Rev. Biomed. Eng.*, 9:133-199.

[8] Hasko, J.A. and Richardson, G.P. (1988). **The ultrastructural organization and properties of the mouse tectorial membrane matrix**. *Hearing Research*, 35:21-38.

[9] Hendrix, D.K. (1990). **Development of an *in vitro* preparation of the alligator lizard cochlear duct**. *M.I.T. Department of Electrical Engineering and Computer Science, Masters Thesis*.

[10] Hudspeth, A.J. (1983). **Mechanoelectrical transduction by hair cells in the acousticolateralis sensory system**. *Ann. Rev. Neurosci.*, 6:187-215.

[11] Holton T., and Hudspeth, A.J. (1983). **A micromechanical contribution to cochlear tuning and tonotopic organization**. *Science*, 222:508-510.

[12] Holton, T., and Weiss, T.F. (1983). **Frequency selectivity of hair cells and nerve fibers in the alligator lizard cochlea**. *J. Physiol.*, 354:241-260.

[13] Kronester-Frei, A. (1978). **Sodium dependent shrinking properties of the tectorial membrane**. *Scanning Electron Microscopy*, 2:943-948.

[14] Kronester-Frei, A. (1979a). **The effect of changes in endolymphatic ion concentrations on the tectorial membrane**. *Hearing Research*, 1:81-94.

[15] Mulroy, M.J. (1974) **Cochlear anatomy of the alligator lizard**. *Brain Behavioral Evolution* 10, 69-87.

[16] Mulroy, M.J. and Williams, R.S. (1986) **Auditory stereocilia in the alligator lizard**. *Hearing Research*, 25:11-21.

[17] Nussbaum, J.H. and Grodzinsky, A.J. (1981). **Proton diffusion reaction in a protein polyelectrolyte membrane and the kinetics of electromechanical forces**. *J. Memb. Sci.*, 8:193-219.

[18] Orman, S.S. and Geisler, C.D. (1986). **Guinea pig tectorial membrane profile in an in vitro cochlear preparation**. *Am. J. Otolaryngol.*, 7:140-146.

[19] Peterson, S.K., Frishkopf, L.S., Lechene, C., Orman, C.M. and Weiss, T.F. (1978). **Element composition of inner ear lymphs of cats, lizards and skates determined by electron probe microanalysis of liquid samples**. *J.Comp Physiol.*, 126:1-14.

[20] Richardson, G.P., Russell, I.J., Duance, V.C. and Bailey, A.J. (1987). **Polypeptide composition of the mammalian tectorial membrane**. *Hearing Research*, 25:45-60.

[21] Ricka, J. and Tanaka, T. (1984). **Swelling of ionic gels: Quantitative performance of the Donnan theory**. *Macromolecules*, 17:2916-2921.

[22] Shah, D., Freeman, D.M., Weiss, T.F. (1994). **The effect of Na^+, K^+, and Ca^{2+} concentration on the isolated, unfixed mouse tectorial membrane**. (Unpublished work).

[23] Steel, K.P. (1983a). **Donnan equilibrium in the tectorial membrane**. *Hearing Research*, 12:265-272.

[24] Steel, K.P. (1983b). **The tectorial membrane in mammals**. *Hearing Research*, 9:327-359.

[25] Sterkers, O., Ferrary, E., and Amiel, C. (1984). **Inter- and intracompartmental osmotic gradients within the rat cochlea**. *Am. J. of Physiol.*, 247:F602-F606.

[26] Sterkers, O., Ferrary, E., and Amiel, C. (1988). **Production of inner ear fluids**. *Physiol. Revs.*, 68:1083-1128.

[27] Tanaka, T. (1981). **Gels**. *Sci. Am.*, 244:124-138.

[28] Thalmann, I., Thallinger, G., Comegys, T.H., Crouch, E.C., Barrett, N. and Thalmann, R. (1987). **Composition and supramolecular organization of the tectorial membrane**. *Laryngoscope*, 97:357-367.

[29] Thalmann, I., Thallinger, G., Comegys, and Thalmann, R. (1986). **Collagen - The predominant protein of the tectorial membrane**. *J. Oto-Rhino-Larynogol.*, 48:106-115.

[30] Weiss, T.F., Mulroy, M.J., Turner, R.G., and Pike, C.L. (1976). **Tuning of single fibers in the cochlear nerve of the alligator lizard: Relation to receptor organ morphology**. *Brain Research*, 115:71-90.